Regulators of Inflammation in Arthritic Disease Pathogenesis

A thesis

submitted by

Daisy Nakamura

In partial fulfillment of the requirements
for the degree of

Doctor of Philosophy

in

Cell, Molecular and Developmental Biology

TUFTS UNIVERSITY

Sackler School of Graduate Biomedical Sciences

August, 2016

Advisor: Li Zeng, PhD

Abstract

Inflammation is a major cause of cartilage destruction and leads to the imbalance of catabolic and anabolic activities in the arthritic joint. Our aim was to investigate both positive and negative regulators of inflammation involved in arthritic joint disease. As a positive regulator, pigment epithelium derived factor (PEDF) has been reported to have both pro- and anti-inflammatory activities in various cell types and shown to be upregulated in the arthritic joint, but its role in joint destruction is unclear. We investigated its role in cartilage degeneration under inflammatory conditions using ectopic PEDF expression in primary human articular knee chondrocytes, explant bone cultures from PEDF-deficient and wild type mice and the monosodium iodoacetate (MIA) inflammatory joint destruction animal model in PEDF-deficient and wild type mice. We showed that PEDF protein expression was higher in human osteoarthritis samples compared to normal samples. We demonstrated that ectopic PEDF expression in primary human articular knee chondrocytes exacerbated catabolic gene expression in the presence of interleukin 1 beta (IL-1β). In whole bone organ cultures, IL-1β induced the expression of matrix metalloproteinase 13 (MMP-13) and caused significant cartilage matrix loss. Interestingly, PEDF-deficient bones from 29 week old animals, but not 10 week old animals, showed reduced MMP-13 protein expression and matrix loss compared to their wild type counterparts. In addition, PEDF-deficiency in 29 week old animals preserved matrix integrity and protected against cell loss in the MIA joint destruction model *in vivo*. We conclude that PEDF exacerbates cartilage degeneration in an age-dependent manner under an inflammatory setting. As a negative regulator, azithromycin (AZM) has exhibited anti-inflammatory activity in various systems and a sister compound, erythromycin, demonstrated chondroprotective effects in an animal model of joint destruction. However, the role of azithromycin in joint destruction has not been investigated. We investigated its role in cartilage degeneration using the MIA inflammatory joint destruction animal model and primary human articular knee chondrocyte cultures in the presence of IL-1β. We found that azithromycin preserved cartilage matrix *in vivo* and inhibited IL-1β-mediated catabolic gene expression *in vitro*. We conclude that AZM has therapeutic potential to treat inflammatory joint disease. Altogether,

these findings broaden our understanding of both positive and negative regulators of inflammation in arthritic disease pathogenesis.

Acknowledgements

I would like to thank my thesis advisor, Dr. Li Zeng, for her support through my thesis work. These past three years have been a blur of activity and I am truly grateful for the opportunity.

I would also like to thank my committee members: Dr. Heber Nielsen, Dr. John Castellot and Dr. John Leong, for keeping me focused and on track. I would also like to thank my external examiner, Dr. Wentian Yang (Brown University) for his time in reviewing this work. I owe a debt of gratitude also to the current and past members of the Zeng laboratory, from the everyday minutia to the big picture discussions. Also, to Jerold Harmatz for his patience and support.

Finally, I would like to thank my family and friends. This journey would not have been possible without them.

Table of Contents

List of Figures

List of Abbreviations

AAAL: arthritis-attributable activity limitations

AZM: azithromycin

Col-II: collagen type II

DAPI: 4',6-diamidino-2-phenylindole dihydrochloride

ECM: extracellular matrix

EM: erythromycin

GAG: glycosaminoglycan

GAPDH: glyceraldhyde-3-phosphate dehydrogenase

GFP: green fluorescent protein

GHSR: growth hormone secretagogue receptor

IGF-I: insulin-like growth factor 1

IHC: immunohistochemistry

Ihh: indian hedgehog

IL-1β: interleukin 1 beta

IL-1Ra: interleukin 1 receptor antagonist

IL-4: interleukin 4

IL-6: interleukin 6

IL-10: interleukin 10

iMAC: immature murine articular chondrocytes

KO: knockout

LV: lentiviral

MCP-1: monocyte chemoattractant protein 1

MIA: monosodium iodoacetate

MMP: matrix metalloproteinase

NF-κB: nuclear factor of kappa light polypeptide gene enhancer in B-cells

NHAC: normal human articular chondrocyte

OA: osteoarthritis

OARSI: Osteoarthritis Research Society International

PEDF: pigment epithelium-derived factor

PBS: phosphate buffered saline

PTHrP: parathyroid hormone-related protein

RA: rheumatoid arthritis

Runx2: runt-related transcription factor 2

SRE: serum response element

TIMP-1: tissue inhibitor of metalloproteinases-1

TNFα: tumor necrosis factor alpha

WT: wild type

1 Introduction

1.1 What is Arthritis?

Arthritis afflicts 52.5 million (22.7%) adults in the US and is a leading cause of disability for whom 22.7 million (9.8% of all adults) experience arthritis-attributable activity limitations (AAAL). By 2040, the prevalence of doctor-diagnosed arthritis is projected to reach 78.4 million (25.9%) adults for whom 34.6 million (11.4% of all adults) will experience AAAL [1]. In 2003, the total cost associated with arthritis was $128 billion of combined medical expenditures and lost earnings [2]. These costs will invariably increase given the projected increases in prevalence.

Arthritis is classified into several subtypes, including osteoarthritis and rheumatoid arthritis, and typically affects joints (e.g. hands, feet, knees, hips), but some forms may also affect multiple organs (e.g. heart, lungs, kidney). Arthritis presents clinically as joint swelling, pain and immobility, ranging from mild intermittent symptoms to severe chronic symptoms. While juveniles also suffer from arthritis, the risk of developing arthritis increases with age. In fact, of the 52.5 million adults reporting doctor-diagnosed arthritis, 49.7% of them are over 65 years of age. Other major non-modifiable risk factors include gender and genetics; women exhibit a higher prevalence than men [3]. Major modifiable risk factors include obesity, joint injury and infection.

Arthritis is a heterogeneous disease with unclear etiology, hampering development of effective treatment options. Patients seeking medical attention have often progressed to fairly late stages of disease, where treatment options are limited to symptomatic relief. While disease-modifying antirheumatic drugs exist for rheumatoid arthritis that slow disease progression [4], current treatment options for the vast majority of arthritis patients do not alter the structural progression of the disease and primarily target pain and inflammation. Joint surgery is a costly alternative that may or may not be an option given the type of arthritis. While new targets for therapy are emerging beyond symptom alleviation for knee osteoarthritis [5], much work remains to address this unmet clinical need. Efforts to develop effective therapeutics are thwarted by an incomplete

understanding of disease progression. To develop disease-modifying agents to treat arthritis, a broader and deeper understanding of its pathogenesis is necessary. This thesis investigates both positive and negative regulators of arthritis of the joint to expand our current understanding of joint arthritis pathogenesis.

1.2 Joint and Inflammation

Inflammation is an important driver of joint disease pathogenesis and affects multiple components of the joint. The most common forms of arthritis are characterized by cartilage matrix destruction, subchondral bone remodeling and inflammation of the synovial membrane, and is becoming recognized as a whole joint disease [6]. These joint components have distinct features that collectively support the joint under normal conditions. To begin understanding joint pathology, one must first understand normal biology.

Articular cartilage is a hyaline tissue found on the surface of articulating bones and serves to lubricate articulating surfaces against friction and absorb compressive forces during joint movement. It is composed of a complex network of proteoglycans and collagen fibrils. While several types of proteoglycans are present, the most abundant is aggrecan, which is largely composed of chondroitin sulfate glycosaminoglycan (GAG) chains. Because of the negative charge of these GAGs, these proteoglycan aggregates draw in water to provide the osmotic resistance to afford cartilage much of its biomechanical properties [7]. In addition to proteoglycans, mature cartilage consists of a network of collagen, which is a fibrous structural protein bundle of three parallel helices and provides cartilage its tensile strength [8]. Collagen makes up 60% of the dry weight of cartilage and contains a variety of collagen types; however, collagen II represents the vast majority, making up 90-95% of the collagen.

Articular cartilage is organized into four zones: superficial or tangential, intermediate or transitional, deep or radial and calcified [9]. The superficial zone makes up approximately 10-20% of the articular cartilage thickness with water contributing to upwards of 80% of the cartilage wet weight. The collagen fibers, which are primarily type II and IX collagen, are aligned largely parallel along the plane of the articular surface [10]. The intermediate zone represents 40-60% of the cartilage volume, where the collagen fibrils are thicker and arranged obliquely. The deep zone makes up approximately 30% of the total articular cartilage volume and can be distinguished by the thickest collagen fibrils in the cartilage and arranged in a vertical orientation. This region provides the most resistance to compressive forces due to its high proteoglycan content and contains approximately 65% water volume. The calcified zone is separated from the deep zone by the tide mark and serves to transition the cartilage to bone by securing the collagen fibrils in the deep zone to the subchondral bone.

Chondrocytes are the specialized cells that reside within the cartilage matrix and exist in an aneural, avascular and low oxygen tension environment. They are generally round cells that are located within matrix cavities called lacunae within the cartilage matrix and represent about 2% of the total cartilage volume [11]. They are metabolically active cells originating from mesenchymal stem cells with limited reparative and replicative capacity. Chondrocytes in the growth plate of long bones play important roles in bone elongation via endochondral ossification, but are mainly responsible for maintaining the dynamic equilibrium of cartilage matrix through anabolism and catabolism of extracellular matrix macro-molecules [10, 12].

Besides cartilage, the joint also includes such elements as ligament, meniscus and synovium. As the majority of this thesis focuses on cartilage, the other joint components will only be briefly described.

Skeletal ligaments are fibrous connective tissue that serves to stabilize the joint by connecting bones to one another. It is composed of approximately two-thirds water and one-third solid, of which collagen type I accounts for the vast majority [13]. In several other joint types, the meniscus is another stabilizing component. It is a semi-lunar fibrocartilaginous structure composed of 72% water by wet weight with extracellular matrix (ECM) and cells constituting the remaining weight. Collagens make up the majority of this ECM, but varies in quantity relative to its respective zone. The major role of the meniscus is in load-bearing, load transmission and shock absorption [14].

The joint synovium or synovial membrane is a connective tissue that lines the inner surface of joint capsules. It provides a deformable structure that can cope with the mechanical strains of joint movement and serves to lubricate cartilage and control synovial fluid volume and composition to nourish chondrocytes interfacing the joint. Under normal conditions, the synovium is composed of two types of synoviocytes: Type A and Type B. Type A synoviocytes exhibit macrophage lineage markers and primarily function to phagocytize debris within the joint. Type B synoviocytes exhibit fibroblast lineage markers and produce hyaluronan, which is crucial for the viscous nature and lubricating properties of synovial fluid that fills the joint space [15, 16].

The joint elements described each play a role in normal joint physiology and can become compromised in the case of arthritis. In osteoarthritis, the most prevalent form of arthritis, there are multiple hallmarks of the disease, which include cartilage matrix degradation, bone remodeling, inflammation, dysfunctional skeletal muscle and a metabolically active adipose tissue that supports disease pathogenesis [17]. This is a common end-stage phenotype where various joint disease subtypes ultimately arrive. The precise sequence of events that leads to joint failure is unclear; in particular, the temporal relationship among synovial inflammation, subchondral bone remodeling and cartilage destruction is not defined. Here, we sought to examine one of these key features in greater depth.

Inflammation is differentially defined depending on the arthritis type. For instance, in rheumatoid arthritis (RA), inflammation is classically defined as having a cellular component represented by leukocyte accumulation in the affected tissues. This is in contrast to osteoarthritis (OA), where inflammation is better recognized on a molecular level in the form of pro-inflammatory mediators, such as cytokines and chemokines. Several inflammatory cytokines are elevated in OA synovial fluid and sera compared to samples from normal healthy donors, suggesting local as well as systemic inflammation. The inflammatory cytokines in OA synovial fluid are higher than OA sera, but both of which are lower than that found in RA, as expected [18].

Elevated leukocytes in classically defined inflammatory arthritis involves both adaptive and innate immune responses and largely reflect cell infiltration rather than local proliferation. The adaptive immune response involves both T and B cells, but the functional role of T cells is unclear despite elevated levels in the inflamed joint. On the other hand, the importance of the humoral adaptive immunity is highlighted by its inclusion in clinical management of patients with inflammatory arthritis. B cells have been extensively studied for their role in autoantibody production, but are becoming recognized for their role in antigen presentation, immune regulation and cytokine production [19]. In addition to the adaptive immune response, innate effector cells such as macrophages, mast cells and natural killer cells that are commonly found in the inflamed synovial membrane are important mediators of disease progression [20]. In particular, macrophages are among the first cell types to traffick to the synovium and release pro-inflammatory cytokines that activate both innate and adaptive systems [21]. Independent of cytokine source, the underlying mechanism of joint inflammation continues to be the release of pro-inflammatory cytokines, as in non-classically defined inflammation. Here, the inflammatory environment is perpetuated by resident cells such as chondrocytes and synoviocytes [22]. Pro-inflammatory cytokines are particularly detrimental to the joint environment in that they upregulate catabolic activities and downregulate anabolic activities that collectively and progressively lead to joint destruction [20, 23]. These will be explored in greater depth in the next section.

1.3 Positive and negative regulators of local joint inflammation

While multiple inflammatory cytokines are elevated in the inflamed joint, a few contribute critically to the disease. Interleukin 1 beta (IL-1β) and tumor necrosis factor alpha (TNFα) are key regulators of inflammation in both classically and non-classically defined inflammation.

Interleukin 1 beta (IL-1β) belongs to a growing complex family of ligands with agonist and receptor antagonist activity [22, 24]. It is produced as an inactive precursor protein that requires intracellular cleavage by caspase-1 to release the active protein into the extracellular space.

IL-1β has been associated with several autoimmune and autoinflammatory diseases and its blockade has been used to treat a variety of inflammatory disease including joint diseases [25]. Upon upregulation in the disease state, IL-1β disrupts the metabolic homeostasis of joint tissues leading to joint disease. In mouse models of osteoarthritis and rheumatoid arthritis, inhibiting IL-1 activity inhibits arthritis progression [26-29]. IL-1β stimulates chondrocytes to release various matrix metalloproteinases (MMPs), including MMP-1, MMP-3 and MMP-13 [30-33], which are key regulators of matrix destruction. In fact, cartilage erosion in a surgical model of OA is dependent on MMP-13 activity [34] and local IL-1 receptor antagonist (IL-1Ra) therapy reduces degenerative changes in the joint in a traumatic injury-induced OA mouse model [26]. However, IL-1β production is not limited to chondrocytes. Osteoblasts, synoviocytes and resident mononuclear cells as well as infiltrated mononuclear cells have also been shown to secrete IL-1β and contribute to disease progression [22, 35]. Despite promising pre-clinical studies in animal models, monotherapy clinical trials with IL-1Ra or monoclonal antibodies targeting the IL-1 receptor have produced variable results for OA [36, 37]. For RA, clinical trials with the IL-1Ra were beneficial only for a subset of the highest dose cohort [38]. This suggests that additional

modulators may collaborate with IL-1β to drive inflammation-associated joint destruction, highlighting the complexity and incomplete understanding of arthritis pathogenesis.

In addition to IL-1β, tumor necrosis factor alpha (TNFα) is another critical factor in inflammatory joint disease [39]. It is a transmembrane protein that is cleaved by the metalloproteinase, TNFα converting enzyme, to release a soluble trimeric cytokine [22, 40, 41]. In the inflamed joint, TNFα is produced by a variety of cell types such as activated macrophages, synovial fibroblasts and osteoclasts to cause chronic inflammation and bone loss [42]. It plays a fundamental role in inflammation as underscored by its clinical application as the first biologic agent approved for the treatment of rheumatoid arthritis [20, 42].

Besides positive regulators of local joint inflammation, anti-inflammatory mediators exist to resolve local inflammation and protect against joint degeneration. One such mediator is interleukin-4 (IL-4), which exhibits chondroprotective effects on cartilage. In inflammatory models of arthritis, IL-4 treatment reduced cartilage proteoglycan damage possibly by the combined effects of reduced MMP activation and enhanced proteoglycan synthesis [22, 43-46]. Another mediator is interleukin-10 (IL-10), which exhibits an array of activities that are chondroprotective. From reducing pro-inflammatory cytokine production to upregulating natural inhibitors of inflammatory cytokines such as IL-1β antagonist and tissue inhibitor of metalloproteinases-1 (TIMP-1), the pleiotropic activities of IL-10 are largely protective [22]. While IL-10 has been shown to be upregulated in human osteoarthritic chondrocytes and in RA patients, it is thought to counteract the degrading effects of catabolic cytokines as it has also been shown to regulate components of the inflammasome [47-49]. In inflammatory models of arthritis, IL-10-deficient animals are more susceptible to joint destruction, while IL-10 treatment reduced cartilage destruction [50, 51].

Because of the early inflammatory component of joint disease pathogenesis, anti-inflammatory therapies could be used to combat disease progression. While direct inhibitors of a specific pro-inflammatory cytokine have shown limited clinical success [36-38], perhaps an anti-inflammatory agent may have the broader scope necessary to interrupt the self-perpetuating inflammatory process that leads to joint disease progression. Alternatively, because of the limited success of monotherapies, perhaps a combination therapy approach such as that used to treat cancer may be necessary. Ultimately, additional agents must be evaluated for potential disease modifying effects and the combination of these therapies should be evaluated to treat this heterogeneous disease.

1.4 Pigment Epithelium Derived Factor as a positive regulator of arthritis

Despite advances in anti-IL-1β research, clinical trials targeting the IL1 receptor or applying the naturally occurring IL1 receptor antagonist have had limited success [36-38]. This suggests that additional modulators may collaborate with IL-1β to drive inflammation-associated joint destruction, highlighting the complexity and incomplete understanding of arthritis pathogenesis.

One such modulator may be pigment epithelium derived factor (PEDF), which is a 50kD secreted glycoprotein belonging to the family of serine protease inhibitors that do not exhibit inhibitory activity [52, 53]. It is expressed in multiple tissues [54-56] and has been extensively studied for its anti-angiogenic and neurotrophic properties as extensively reviewed previously [54, 57-62]. It has been shown to bind cartilage matrix components, making its localization possibly functionally relevant [63-65].

One key feature of PEDF as it relates to joint physiology is its activity on bone homeostasis. PEDF treatment directs murine and human mesenchymal stem cell fate determination towards osteoblasts [66, 67], which is critical for bone mineralization. In fact, PEDF knockout animals

exhibit reduced trabecular bone volume and diminished bone mineralization [66, 68] likely because PEDF suppresses the expression of factors that inhibit mineralization and enhance those that promote mineralization [69]. PEDF activity is not limited to osteoblasts as it has also been shown to regulate osteoclast differentiation, survival and bone resorption [70]. Thus, PEDF activity on bone homeostasis involves multiple elements.

Another important feature of PEDF is its ability to modulate the inflammatory response in a variety of systems. For example, systemic expression of PEDF in diabetic rats led to a reduction in tumor necrosis factor alpha (TNFα) and monocyte chemoattractant protein 1 (MCP-1) expression in the retina as well as the kidney [71, 72]. On the other hand, in skeletal muscle cells and neonatal astrocytes, PEDF treatment activated the inflammatory mediator, nuclear factor of kappa light polypeptide gene enhancer in B-cells (NF-kB) [73, 74].

In arthritic disease pathogenesis, the role of PEDF is unclear as even its expression in the joint is controversial. In one report, PEDF expression is found in normal articular chondrocytes and upregulated in human OA cartilage samples [75]. On the other hand, a recent study shows that PEDF is not expressed in normal or OA articular chondrocytes, but is only upregulated predominantly in osteophytic chondrocytes [76]. While it was shown that PEDF contributes to the terminal differentiation of the endochondral ossification process of osteophyte formation [76], its role in the inflammatory process in joint destruction remains insufficiently understood. We sought to investigate PEDF expression in articular chondrocytes, and address whether PEDF plays a role in cartilage degeneration by evaluating its effects on cartilage in an *ex vivo* culture system under inflammatory stimuli and in an inflammatory animal model of joint destruction.

1.5 Azithromycin as a negative regulator of arthritis

Azithromycin belongs to the macrolide class of antibiotics, which is so named for the macrocyclic lactone ring structure. It is a semi-synthetic derivative of erythromycin, which was the first macrolide antibiotic to be identified. Azithromycin (AZM) has an extended elimination half-life of 68hrs compared to the 3hrs for erythromycin (EM) [77]. This is likely due to the fact that AZM is not metabolized by cytochrome P450 3A4, which is an important enzyme that oxidizes small foreign organic molecules for removal from the body. Another key feature of AZM is the fact that it is readily taken up by phagocytic cells in a non-saturable manner [78, 79], which is critical for its local delivery to sites of inflammation [80-82].

Originally identified for its bactericidal and bacteriostatic activity, macrolide antibiotics have recently shown anti-inflammatory activity in various systems. They have been especially successful in the management of chronic respiratory diseases such as diffuse panbronchiolitis and cystic fibrosis [83]. Its anti-inflammatory activity is multifactorial. Not only do macrolides modulate immune cell function, they also inhibit the bacterial biofilm production important in lung infections of cystic fibrosis patients [83-86]. In addition to respiratory diseases, macrolides have also been effective at treating skin disorders [87].

In an experimental murine model of arthritis, we have previously shown that erythromycin exhibits chondroprotective effects. Erythromycin treatment protected murine joints from cartilage matrix loss and synovitis. Additionally, erythromycin inhibited IL-1β-induced expression of MMPs in articular chondrocytes [88]. Further work has shown that erythromycin binds to the ghrelin receptor and can be functionally blocked in murine chondrocytes lacking the ghrelin receptor (unpublished data). Because of these promising results, we sought to determine whether other macrolides also exhibit chondroprotective effects in our murine model and anti-inflammatory activity in chondrocyte cell cultures and chose azithromycin based on its extended elimination half-life and targeted delivery. To do so, we evaluated the effects of azithromycin on articular chondrocytes under inflammatory stimuli and in an inflammatory animal model of joint destruction.

1.6 Summary

The heterogeneous nature of arthritis lends to the complexity and incomplete understanding of its pathophysiology. Current therapeutics primarily offer symptomatic relief from end-stage disease without a clear path toward disease-modifying agents. A better understanding of disease pathophysiology is necessary. To probe deeper into the disease, we sought to address both positive and negative regulators of inflammation in joint degeneration.

Because PEDF is upregulated in the disease state, we hypothesized that PEDF synergizes with inflammatory stimuli to exacerbate the catabolic response in chondrocytes, leading to elevated matrix degradation in an inflammatory joint destruction model *in vivo*. To determine whether PEDF plays a role in regulating cartilage degeneration, we evaluated its effects on cartilage in an *ex vivo* culture system under inflammatory stimuli and in an inflammatory animal model of joint destruction. We demonstrated that PEDF potentiates inflammatory stimuli-induced joint cartilage damage. PEDF enhanced the catabolic gene profile of primary human articular chondrocytes under inflammatory stimuli. In explant cultures using PEDF-deficient mice, loss of PEDF expression protected older explant cultures from matrix loss, which was associated with a decrease in MMP-13 expression. In an *in vivo* inflammatory joint destruction model, PEDF loss preserved matrix levels and cellularity. Thus, PEDF in an inflammatory disease state potentiates joint degeneration in an age-dependent manner.

Because azithromycin belongs to the same macrolide class of antibiotics as erythromycin, we hypothesized that it protects against cartilage matrix loss, synovitis and cell loss in an inflammatory joint destruction model *in vivo*. To determine the anti-inflammatory activity of azithromycin in the joint, we evaluated its effects on cartilage in an inflammatory animal model of joint destruction and in an *in vitro* culture system under inflammatory stimuli. We found that

azithromycin inhibits monosodium iodoacetate (MIA)-induced cartilage matrix loss *in vivo* and inhibited IL-1β-mediated catabolic gene expression in chondrocyte cultures.

These findings broaden our understanding of both the positive and negative regulators of inflammatory joint disease. With pigment epithelium derived factor, we begin to appreciate additional molecular insight into the age-related prevalence of joint diseases. And while much work still remains for azithromycin, we explore further the use of antibiotics as an anti-inflammatory therapeutic against inflammatory joint disease progression.

2 Materials and Methods

2.1 PEDF under inflammatory conditions

Normal and OA Human Cartilage Specimens

Normal human articular cartilage slices were isolated from the tibial plateau of cadaveric joints obtained from the National Disease Research Interchange. Human OA tibial plateau were obtained from patients undergoing total knee replacement surgery at Tufts Medical Center. Donors consisted of the following: 54 year old female, 67 year old male, 53 year old female. To confirm the integrity of the articular cartilage, histological specimens were scored using the Mankin system [89].

Generating Lentiviral Constructs

The full length human PEDF sequence and tdTomato sequence were amplified with P2A-sequence containing primers. Overlapping sequences of human PEDF-P2A and P2A-tdTomato were used in Gibson Assembly with the pWPXLd lentiviral backbone (Addgene), targeting PEDF-P2A-tdTomato downstream of the EF-1α promoter. Similarly, the GFP sequence was amplified with P2A-sequence containing primers. Overlapping GFP-P2A and P2A-tdTomato sequences were used in Gibson Assembly with the pWPXLd lentiviral backbone for use as a transduction control.

Cell Culture and Reverse Transcriptase-Polymerase Chain Reaction (RT-PCR) Analysis

Primary normal human knee articular chondrocytes (Lonza) were redifferentiated in alginate beads according to the manufacturer's protocol using chondrogenic differentiation medium (Lonza). Redifferentiated normal human knee articular chondrocytes were transduced with lentiviruses encoding GFP or PEDF for 48hrs then cultured for 4 days in chondrogenic differentiation medium in the presence or absence of 1ng/mL of interleukin-1β (IL-1β) (PeproTech). Total RNA from cultured chondrocytes was isolated using the RNeasy Mini Kit

(Qiagen), and complementary DNA was generated using Moloney Murine Leukemia Virus Reverse Transcriptase (Invitrogen). Quantitative PCR was performed using an iQ5 Real-Time PCR Detection System (Bio-Rad). All RT-PCR analyses were normalized to TATA box binding protein mRNA expression [90].

Western Blot Analysis

Redifferentiated primary normal human knee articular chondrocytes (Lonza) were transduced with lentiviruses encoding GFP or PEDF for 72hrs. Normal human articular chondrocytes were lysed using the standard RIPA buffer. Nuclear and cytoplasmic fractions were obtained using NE-PER Nuclear and Cytoplasmic Extraction Reagents (Pierce) according to manufacturer instructions. Protein concentrations were determined using the DC Protein Assay (Bio-Rad). Cytoplasmic fraction proteins (5µg) were loaded. Primary and secondary antibodies: rabbit anti-PEDF (BioProductsMD), mouse anti-α-tubulin (DSHB, 12G10) and goat anti-rabbit or mouse IgG, (H+L) HRP conjugate (Millipore/Chemicon).

Enzyme-linked immunosorbent assay (ELISA)

TC28a/2 cells were transduced with lentiviruses encoding for PEDF or GFP. Stably-transduced cells were plated on 48-well plates for 48hrs and supernatant was harvested for ELISA. Samples were normalized to total DNA content. To measure DNA content, cells were lysed in 350µl RLT Buffer (Qiagen) [91] for DNA quantification using the Quant-iT PicoGreen dsDNA Assay Kit (Invitrogen) according to the manufacturer instructions. Secreted PEDF protein levels were assessed using the Human Serpin F1 ELISA kit (RayBiotech) according to manufacturer instructions.

Animals and MIA Injection

All animal care and experimental procedures were approved by the Institutional Animal Care and Use Committee at Tufts University. PEDF-deficient mice were a generous gift from Regeneron to Dr. H. Nielsen (Tufts University) and has been described previously [56, 92, 93]. Mice were housed in groups under standard conditions with a 12-hour light/dark cycle and allowed *ad libitum* access to standard chow and water. 29 week old mice were anesthetized by isoflurane/O_2 inhalation and received a single intraarticular injection of monosodium iodoacetate (MIA) (Sigma) using a 30G ½" needle with 50µg MIA dissolved in 5µL of sterile PBS. PBS-injected contralateral knees served as a negative control. Knees were harvested 10 days post-injection.

Metatarsal Bone Culture

Metatarsal bones from 10 or 29 week old wild type or PEDF-deficient mice were harvested and the second, third and fourth metatarsal bones were cultured in the presence or absence of 10ng/mL IL-1β for 7 days in Dulbecco's Modified Eagle Medium (Invitrogen) supplemented with 0.25% FBS, 0.28% Ascorbic Acid, 0.25% Sodium Pyruvate and 1% Antibiotic-Antimycotic (Invitrogen). Media was replaced every 48 hours.

Immunohistochemistry

For the evaluation of human articular cartilage, sections were stained with 0.1% Safranin O and counterstained with Fast Green and Hematoxylin. For PEDF staining, sections were treated sequentially with both heat-mediated and enzymatic antigen retrieval using 10mM Sodium Citrate, pH 6.0 and 0.3% hyaluronidase supplemented with 0.15% trypsin-EDTA, respectively. Samples were blocked in 10% goat serum in PBS, followed by mouse anti-PEDF (Chemicon, 10F12.2) incubation overnight. Biotinylated mouse IgG was used as a secondary antibody. PEDF expression was detected using the Vectastain ABC Kit with DAB Peroxidase Substrate Kit (Vector Laboratories). Samples were counterstained with 0.5% Methyl Green in 0.1M Sodium Acetate.

For the evaluation of mouse knees, isolated joints were fixed in 1% paraformaldehyde in PBS overnight at 4°C, decalcified in 0.33M EDTA, embedded in paraffin and sectioned sagittally at 5μm thickness. For histological analysis, sections were stained with 0.1% Safranin O and counterstained with Fast Green and Hematoxylin. For PEDF staining, sections were sequentially treated with both heat-mediated and enzymatic antigen retrieval using 10mM Sodium Citrate, pH 6.0 and 0.3% hyaluronidase supplemented with 0.15% trypsin-EDTA, respectively. Samples were blocked with M.O.M. Mouse IgG Blocking Reagent (Vector Laboratories) per manufacturer instructions, followed by mouse anti-PEDF (Chemicon, 10F12.2) incubation overnight. PEDF expression was detected using an Alexa Fluor 594 Goat anti-mouse secondary (Jackson ImmunoResearch Laboratories) and nuclei were stained with DAPI (Roche).

For the evaluation of metatarsal bones, samples were fixed in 1% paraformaldehyde in PBS overnight at 4°C, decalcified in 0.33M EDTA, embedded in O.C.T. (Tissue-Tek) and cryosectioned at 5μm thickness. Sections were stained with 0.4% Toluidine Blue in 0.1M Sodium Acetate where shown. For PEDF staining, sections were treated sequentially with both heat-mediated and enzymatic antigen retrieval using 10mM Sodium Citrate, pH 6.0 and 0.3% hyaluronidase supplemented with 0.15% trypsin-EDTA, respectively. Samples were blocked with M.O.M. Mouse IgG Blocking Reagent (Vector Laboratories) per manufacturer instructions, followed by mouse anti-PEDF (Chemicon, 10F12.2) incubation overnight. PEDF expression was detected using the Vectastain ABC Kit with DAB Peroxidase Substrate Kit (Vector Laboratories). Samples were counterstained with 0.5% Methyl Green in 0.1M Sodium Acetate. For MMP-13 staining, sections were incubated with 0.3% hyaluronidase in PBS supplemented with 0.15% trypsin-EDTA for enzymatic antigen retrieval. Tissues were blocked with M.O.M. Mouse IgG Blocking Reagent (Vector Laboratories) per manufacturer instructions. Mouse anti-MMP-13 (Abcam, VIIIA2) was incubated overnight, followed by Biotinylated Mouse IgG (Vector

Laboratories) and DyLight 594 Streptavidin (Vector Laboratories). Nuclei were stained with DAPI (Roche).

Bright-field and fluorescent images were taken using an Olympus IX-71 inverted microscope and an Olympus DP70 digital camera.

Histological Analysis

Images were randomized and blindly scored using the ImageJ software. For percent cartilage matrix loss along the articular surface, the length of regions exhibiting a loss of Toluidine Blue staining along the articular surface were measured. The sum of these lengths was divided over the total articular surface length to obtain a percent surface area loss. For percent positive area, regions of interest were drawn around the articular cartilage and percent positive areas of MMP-13 staining were calculated. Using the Osteoarthritis Research Society International (OARSI) histological scoring system, OARSI scores were tallied according to the modified scoring system previously described for models with limited structural damage [94]. Percent cell loss was calculated by comparing DAPI stained images to bright-field images [88]. Total cell numbers combined DAPI positive numbers and lacunae numbers void of DAPI staining within the articular cartilage. Percent cell loss was calculated from empty lacunae numbers over total cell number.

Statistical Analysis

Data are plotted as mean ± SEM. Parametric and non-parametric statistical analyses were employed where appropriate. Student's t-test was used for parametric data and Mann-Whitney test was used for non-parametric data. All statistical analyses were performed using Prism (GraphPad Software). P-values of < 0.05 are considered statistically significant.

2.2 Azithromycin and inflammatory joint disease

Animals

All animal care and experimental procedures were approved by the Institutional Animal Care and Use Committee at Tufts University. Mice were housed in groups under standard conditions with a 12-hour light/dark cycle and allowed *ad libitum* access to standard chow and water.

Tissue Penetration Study

For the azithromycin (AZM) tissue penetration study, 10 week old C57bl/6 male mice received a single subcutaneous injection of 10 or 50mg/kg of azithromycin or PBS vehicle control. Because azithromycin is dissolved in 100% ethanol, PBS vehicle control used the ethanol concentration corresponding to the 50mg/kg dose. Blood serum and knees were collected at 1 and 6hrs post-injection. Isolated serum and knees were frozen for azithromycin analysis by mass spectrometry in Dr. David Greenblatt's lab.

Monosodium Iodoacetate (MIA) Model

For the inflammatory joint destruction model, 12 week old C57bl/6 mice were anesthetized by isoflurane/O_2 inhalation and received a single intraarticular injection of MIA (Sigma) using a 30G½" needle with 60µg MIA dissolved in 6µL of sterile PBS. PBS-injected contralateral knees served as a negative control. Respective treatment groups received daily subcutaneous injections of 50mg/kg/d of azithromycin or vehicle control for 7 days beginning the day of MIA injection. Knees were harvested 7 days post-injection.

Immunohistochemistry

Isolated joints were fixed in 1% paraformaldehyde in PBS overnight at 4°C, decalcified in 0.33M EDTA, embedded in paraffin and sectioned sagittally at 5μm thickness. Sections were stained with 0.1% Safranin O and counterstained with Fast Green and Hematoxylin.

Histological Analysis

Image analysis was performed using the ImageJ software. For percent cartilage area loss, regions of interest were drawn around the articular cartilage and percent positive areas of Safranin O staining were calculated using a color threshold exclusion of colors outside the red peak. Using the Osteoarthritis Research Society International (OARSI) histological scoring system, OARSI scores were tallied according to the modified scoring system previously described for models with limited structural damage [94]. Percent cell loss was calculated by comparing DAPI stained images to bright-field images [88]. Total cell numbers combined DAPI positive numbers and lacunae numbers void of DAPI staining within the articular cartilage. Percent cell loss was calculated from empty lacunae numbers over total cell number. Synovitis was scored according to previously established methods [95].

Cell Culture and Reverse Transcriptase-Polymerase Chain Reaction (RT-PCR) Analysis

Primary normal human knee articular chondrocytes (Lonza) were redifferentiated in alginate beads according to manufacturer instructions using chondrogenic differentiation medium (Lonza). For gene expression studies, normal human articular chondrocytes (NHAC) dissociated from alginate beads were pre-treated with azithromycin for 48hrs followed by treatment with or without 1ng/mL of interleukin-1β (IL-1β) (PeproTech). Total RNA from cultured chondrocytes was isolated using the RNeasy Mini Kit (Qiagen), and complementary DNA was generated using Moloney Murine Leukemia Virus Reverse Transcriptase (Invitrogen). Quantitative PCR was performed using an iQ5 Real-Time PCR Detection System (Bio-Rad). All RT-PCR analyses were normalized to TATA box binding protein mRNA expression [90].

Toxicity Assay

Redifferentiated NHAC dissociated from alginate beads were treated with azithromycin or monosodium iodoacetate for 48hrs in chondrogenic differentiation medium for cell viability studies using the Live/Dead Viability/Cytotoxicity Kit (Molecular Probes) according to manufacturer instructions. Total live cells were counterstained with Hoechst nuclear dye and images were quantified using ImageJ.

Glucose Uptake Assay

Redifferentiated NHAC embedded in alginate beads were pre-treated with AZM for 24hrs, followed by MIA for 18hrs. Glucose uptake was assessed after 30mins incubation with 100μg/mL fluorescently-tagged glucose derivative (2-NBDG). Readout values were normalized to DNA as determined by Hoechst counterstain. Percent glucose uptake was calculated relative to vehicle-treated controls.

Glucose Consumption Assay

Redifferentiated NHAC dissociated from alginate beads were pre-treated with AZM for 24hrs, followed by MIA for 48hrs. Glucose consumption was assessed from 3μl media supernatant and incubated with 125μl assay reagent. Readout values were normalized to DNA content per well. To measure DNA content, cells were lysed in 350μl RLT Buffer (Qiagen) [91] for DNA quantification using the Quant-iT PicoGreen dsDNA Assay Kit (Invitrogen) according to the manufacturer instructions. Glucose consumption was compared relative to vehicle-treated controls.

Immature Murine Articular Chondrocytes

Immature murine articular chondrocytes (iMAC) were isolated as previously described [96]. Briefly, postnatal day 6 pups from Ghrelin receptor knockout (GHSR-KO) mice or wild type (WT) littermates were genotyped such that femoral condyles and tibial plateaus could be isolated and pooled accordingly. Cartilage pieces were digested with collagenase at 37°C for 45mins and digestion buffer exchanged for a second 45mins incubation. Digestion buffer was again exchanged and cartilage pieces were incubated overnight. Isolated chondrocytes were either frozen as primary cells or expanded for 6-7 days in culture with DMEM supplemented with 10% FBS and 1% antibiotic/antimycotic.

Statistical Analysis

Data are plotted as mean ± SEM. Parametric and non-parametric statistical analyses were employed where appropriate. Student's t-test was used for parametric data and Mann-Whitney test was used for non-parametric data. For multiple comparisons, the Kruskal-Wallis test was employed with Dunn's Multiple Comparison test. All statistical analyses were performed using Prism (GraphPad Software). P-values of < 0.05 are considered statistically significant.

3 Results

3.1 PEDF under inflammatory conditions

3.1.1 PEDF overexpression potentiates the catabolic effect of IL-1β in human primary articular chondrocytes

Because of the controversy surrounding PEDF expression in chondrocytes, we first performed immunohistochemistry to assess its expression. We obtained articular cartilage samples from cadaveric knees of normal healthy subjects and osteoarthritis (OA) samples from patients undergoing total knee replacement surgery. Because healthy cartilage is avascular and aneural and tissues were harvested within 24hrs postmortem, we do not expect much loss in tissue integrity between normal cadaveric knees and samples isolated from patients undergoing surgery.

When stained for histological analysis, OA samples that exhibited greater cartilage matrix loss, as indicated by reduced Safranin O staining, scored higher on the Mankin scale, which classifies samples according to OA histopathology [89] (Figure 3.1.1a, c). Samples with greater damage demonstrated elevated PEDF protein levels compared to normal control samples (Figure 3.1.1b, d), supporting the notion that PEDF is elevated in OA articular chondrocytes [75].

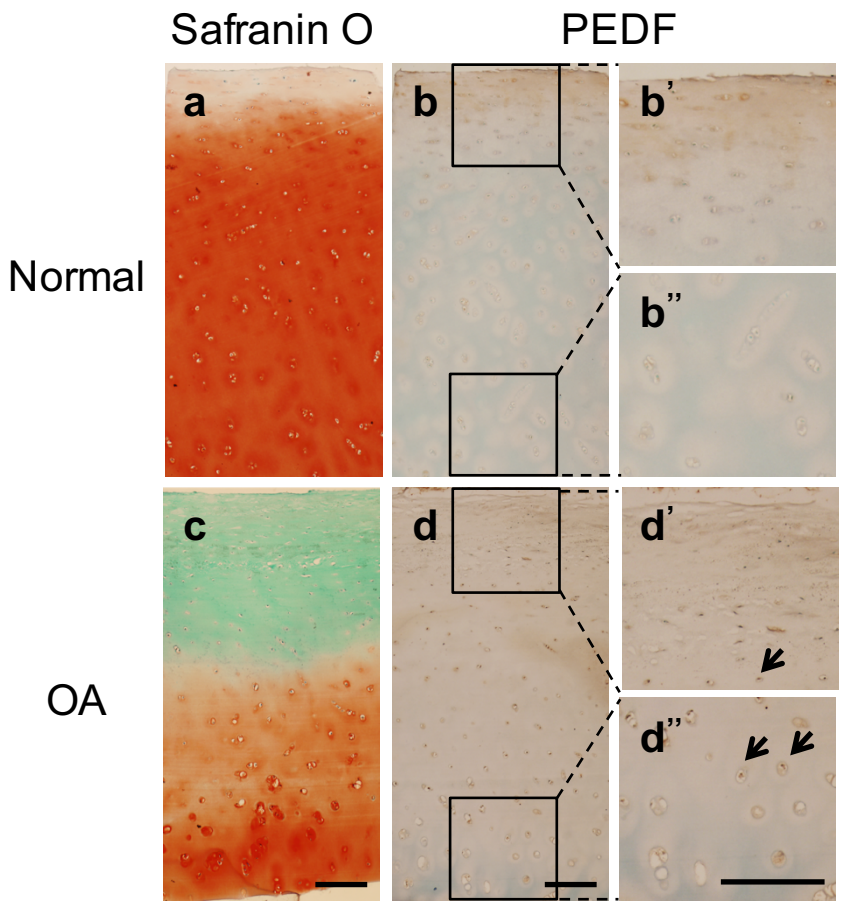

Figure 3.1.1 PEDF expression is elevated in human osteoarthritis (OA) cartilage specimens.

Normal samples were obtained from National Disease Research Interchange and OA samples were obtained from patients undergoing total knee replacement surgery. (a) Normal sample stained with Safranin O and counterstained with Hematoxylin and Fast Green. Mankin score = 1. (b) Immunohistochemistry (IHC) analysis on a normal cartilage sample using a mouse anti-PEDF antibody and counterstained with Methyl Green. Magnified superficial and deeper zones are shown from insets. (c) OA sample stained with Safranin O and counterstained with Hematoxylin and Fast Green. Mankin score = 5. (d) IHC analysis on an OA sample using a PEDF antibody and counterstained with Methyl Green. Magnified superficial and deeper zones are shown from insets. Arrows indicate positive PEDF staining. Scale bar = 200μm.

To determine the effects of elevated PEDF levels, we generated lentiviral expression vectors encoding human PEDF and a tdTomato moiety separated by a P2A self-cleaving peptide. A lentiviral expression vector encoding green fluorescent protein (GFP) served as a transduction control (Figure 3.1.2a). We obtained comparable lentiviral expression for the PEDF and control expression vectors in normal human knee articular chondrocytes (NHAC), which was associated with elevated PEDF protein expression from cellular lysates (Figure 3.1.2b-c). The PEDF protein

was secreted, as determined by PEDF ELISA on the supernatant of transduced cells (data not shown). Using these lentiviral vectors, we investigated the role of PEDF in chondrocytes under inflammatory conditions by transducing NHAC with lentiviral-PEDF followed by treating with 1ng/mL of the pro-inflammatory cytokine, interleukin-1β (IL-1β), for 4 days. In the absence of IL-1β, PEDF overexpression alone slightly elevated the expression of catabolic genes (MMP-1, MMP-3 and MMP-13) relative to GFP-transduced control NHAC. While IL-1β treatment significantly elevated catabolic gene expression in the GFP-transduced control cells, additional ectopic PEDF expression synergized with IL-1β, leading to further elevation of catabolic gene expression (Figure 3.1.2d). This result suggests that PEDF potentiates the catabolic effect of IL-1β.

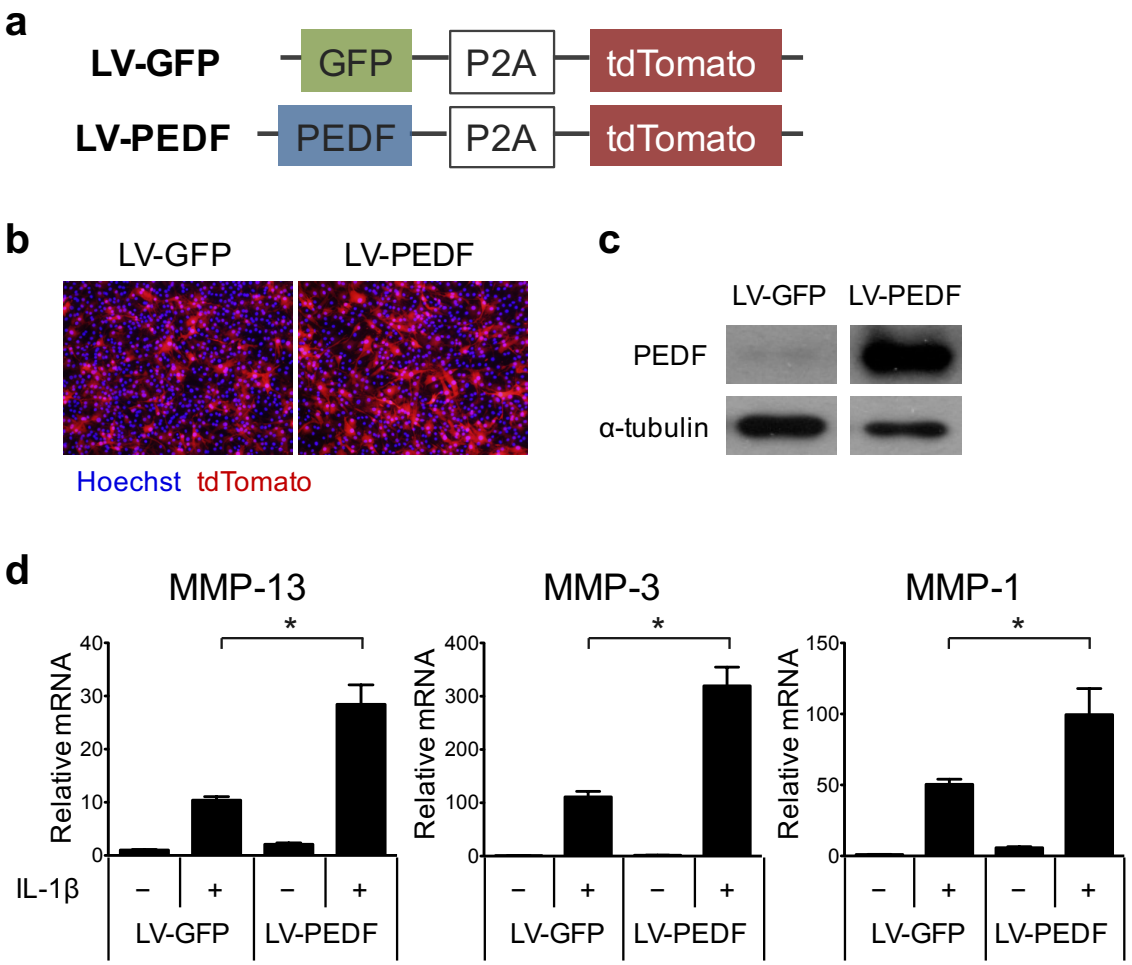

Figure 3.1.2 PEDF ectopic expression upregulates catabolic gene expression in normal human articular chondrocytes (NHAC).

(a) Lentiviral expression vectors were generated to ectopically express PEDF. GFP was used as a control. Both expression vectors also expressed a tdTomato moiety separated by a self-cleaving P2A peptide. (b) tdTomato expression is comparable between the two expression vectors. (c) Western blot analysis confirmed elevated PEDF protein levels in the cytoplasmic fraction of PEDF-transduced NHAC. α-tubulin was used as a loading control. LV-GFP: GPF-encoding lentivirus; LV-PEDF: PEDF-encoding lentivirus. (d) Transduced NHAC were cultured in the presence or absence of 1ng/mL IL-1β for 4 days. Data are represented as fold change relative to GFP-transduced cells in the absence of IL-1β within each gene. Gene expression was normalized to TATA-binding protein mRNA expression levels. Data are plotted as mean ± SEM. * $p < 0.05$ (Mann-Whitney test).

3.1.2 PEDF is required to potentiate IL-1β-induced cartilage matrix loss in articular cartilage

To examine whether PEDF played a similar role in chondrocytes embedded in their native cartilage environment, we sought to evaluate matrix levels in metatarsal bones from wild type and PEDF-deficient mice challenged with inflammatory stimuli. Because age is a major risk factor for arthritis, we evaluated metatarsal bones from two different ages, one of early adulthood (10 weeks old) in the mouse and one of later adulthood (29 weeks old). We opted to culture metatarsal bones for their ease of organ culture and susceptibility to inflammation-mediated arthritic damage in culture [97-100].

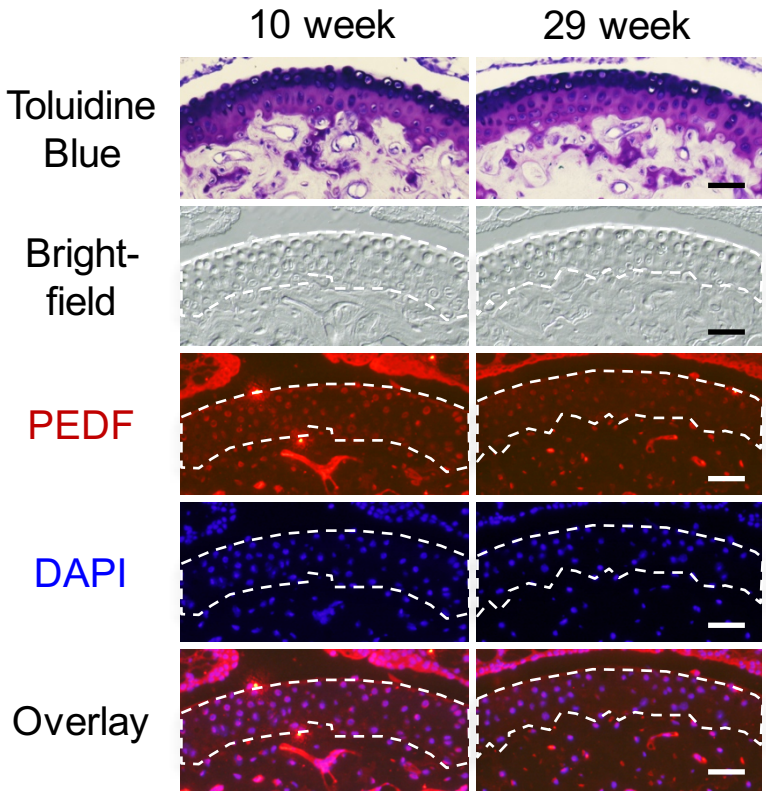

Figure 3.1.3 PEDF is expressed in the articular surface of adult mouse metatarsal bones.
Metatarsal bones from 10 and 29 week old mice were subjected to Toluidine Blue staining and immunohistochemistry (IHC) analysis using a mouse anti-PEDF antibody. Nuclei were counterstained with DAPI. Scale bar = 200μm.

We first confirmed that PEDF expression was found in the articular chondrocytes of metatarsal bones of both 10 and 29 week old mice (Figure 3.1.3). We next performed Toluidine Blue staining to evaluate cartilage matrix levels. Our result indicated no difference in cartilage matrix levels of

either wild type or PEDF-deficient explant cultures in the absence of IL-1β treatment. However, in the presence of IL-1β, samples from both 10 and 29 week old mice demonstrated a loss of Toluidine Blue staining along the articular surface (Figure 3.1.4a, c). Quantification of percent surface area loss of staining upon IL-1β treatment showed no statistically significant difference between PEDF-deficient mice and their wild type counterparts when samples were isolated from 10 week old mice (Figure 3.1.4b). Strikingly, we observed significantly lower levels of cartilage matrix loss in the PEDF-deficient samples that were isolated from 29 week old mice compared to their wild type counterparts, suggesting that PEDF-deficiency attenuated this loss of staining in samples from older mice under inflammatory conditions (Figure 3.1.4d). Additionally, cartilage matrix loss was significantly greater in wild type samples isolated from 29 week old mice (mean of 61%) compared to 10 week old mice (mean of 49%), supporting the notion that older animals are more susceptible to damage (Figure 3.1.4b, d).

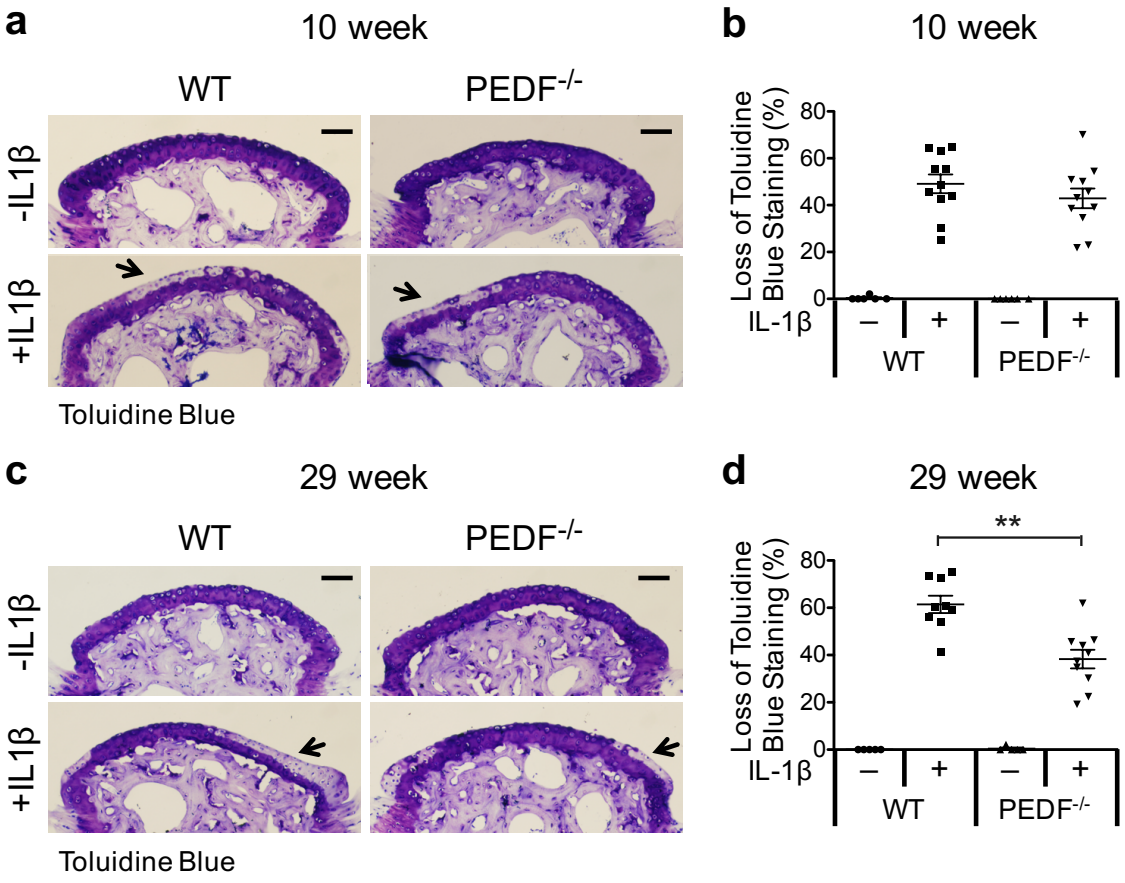

Figure 3.1.4 PEDF-deficiency protects against IL-1β-induced matrix loss in organ cultures of metatarsal bones.

(a) Metatarsal bones from 10 week old wild type or PEDF-deficient mice were harvested and cultured in the presence or absence of 10ng/mL IL-1β for 7 days. Samples were cryosectioned and stained with Toluidine Blue. Arrows indicate areas along the articular surface sustaining a loss of staining. Scale bar = 100μm. (b) Percent surface area loss for 10 week old samples was calculated against total surface area along the articular surface and plotted for each metatarsal bone. Each point represents an individual metatarsal bone with samples pooled from three independent animals. Data are plotted as mean ± SEM. (c) Metatarsal bones from 29 week old wild type or PEDF-deficient mice were harvested and cultured in the presence or absence of 10ng/mL IL-1β for 7 days. Samples were cryosectioned and stained with Toluidine Blue. Arrows indicate areas along the articular surface sustaining a loss of staining. Scale bar = 100μm. (d) Percent surface area loss for 29 week old samples was calculated against total surface area along the articular surface and plotted for each metatarsal bone. Each point represents an individual metatarsal bone with samples pooled from three independent animals. Data are plotted as mean ± SEM. ** p = 0.0021 (Mann-Whitney test).

We next assessed MMP-13 expression within the articular cartilage. As expected, neither wild type nor PEDF-deficient samples expressed MMP-13 within the articular cartilage in the absence of IL-1β. However, in the presence of inflammatory stimuli, significant levels of MMP-13 were

induced (Figure 3.1.5a, c). Significantly, articular cartilage from 10 week old PEDF-deficient mice expressed similar levels of MMP-13 to their age-matched wild type controls under IL-1β treatment (Figure 3.1.5a-b), while articular cartilage from 29 week PEDF-deficient mice expressed lower levels of MMP-13 compared to their wild type counterparts (Figure 3.1.5c-d). These data are consistent with the Toluidine Blue analysis, showing that PEDF exaggerated the response to IL-1β in older animals and suggests that its presence rendered cells to be more responsive to inflammatory stimuli over time.

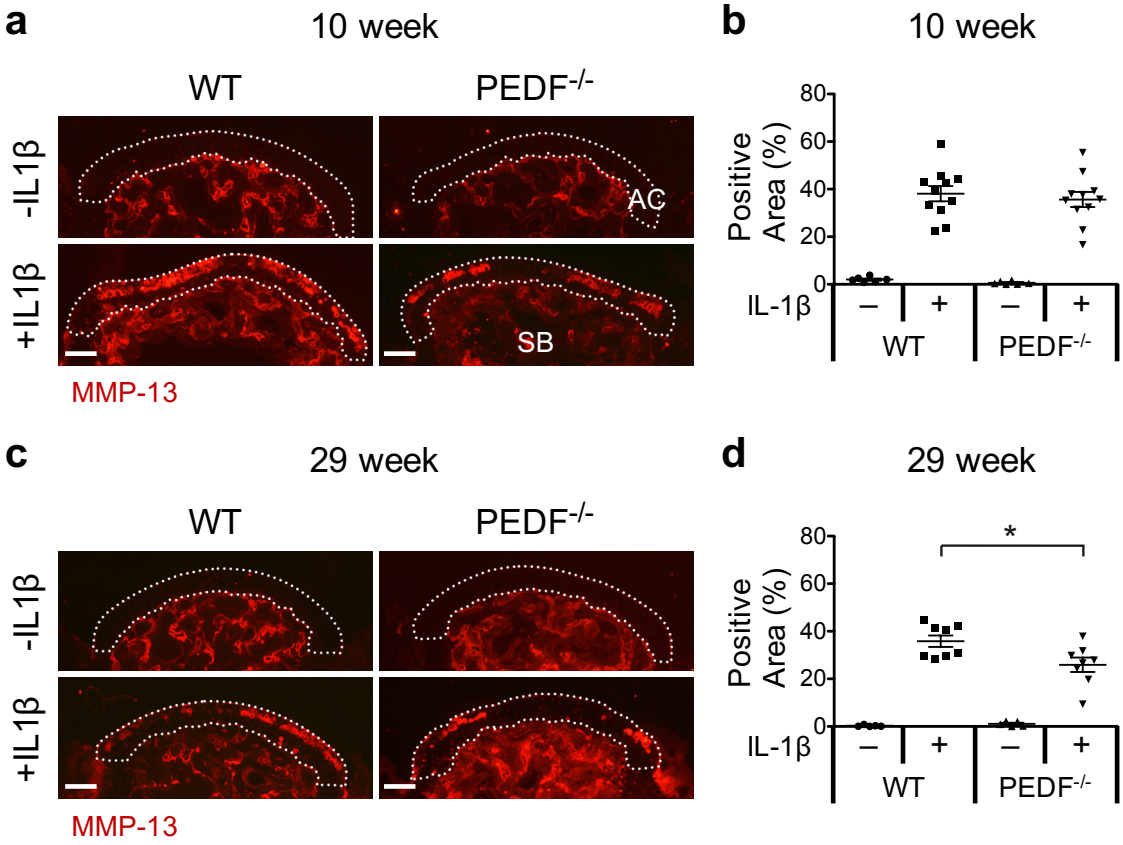

Figure 3.1.5 PEDF-deficiency protects against IL-1β-induced MMP-13 expression in organ cultures of metatarsal bones.

(a) Metatarsal bones from 10 week old wild type or PEDF-deficient mice were harvested and cultured in the presence or absence of 10ng/mL IL-1β for 7 days. Samples were cryosectioned and MMP-13 expression determined via immunofluorescence staining. Arrows indicate areas along the articular surface expressing MMP-13 protein. Scale bar = 100μm. (b) The percent positive area along the articular surface for 10 week old samples was calculated against the total articular surface area and plotted for each metatarsal bone. Each point represents an individual metatarsal bone with samples pooled from three independent animals. Data are plotted as mean ± SEM. AC: articular cartilage; SB: subchondral bone. (c) Metatarsal bones from 29 week old wild type or PEDF-deficient mice were harvested and cultured in the presence or absence of 10ng/mL IL-1β for 7 days. Samples were cryosectioned and MMP-13 expression determined via immunofluorescence staining. Arrows indicate areas along the articular surface expressing MMP-13 protein. Scale bar = 100μm. (d) The percent positive area along the articular surface for 29 week old samples was calculated against the total articular surface area and plotted for each metatarsal bone. Each point represents an individual metatarsal bone with samples pooled from three independent animals. Data are plotted as mean ± SEM. * p = 0.0281 (Mann-Whitney test).

3.1.3 PEDF is required to potentiate joint cartilage damage in an inflammatory joint destruction model *in vivo*

We next evaluated the role of PEDF in regulating cartilage integrity *in vivo* using the monosodium iodoacetate (MIA) model. MIA is a specific inhibitor of glycolysis, which causes cell death and induces joint inflammation and cartilage damage [88]. Because we observed a protective effect of PEDF-deficiency in the older animals (29 weeks old) of our organ cultures, we evaluated the role of PEDF *in vivo* using animals of this age.

While it would be interesting to evaluate PEDF in an *in vivo* model over an extended time frame, we instead chose to use a shorter term *in vivo* model, as global PEDF-deficient animals exhibit lower bone mineral density [66-68, 70], which may influence articular cartilage physiology in long-term studies. The MIA model did not exhibit any appreciable structural damage (such as clefts) in the joint of either wild type or PEDF-deficient animals within the time frame of our studies. Nevertheless, to more closely model arthritis, a slowly progressing model would be ideal. Thus, generating a conditional PEDF knockout and analyzing its role using multiple joint destruction models over longer time frames would be important to distinguish its roles in cartilage and bone pathogenesis.

We first confirmed that PEDF was expressed in the articular chondrocytes of the mouse knee joint (Figure 3.1.6a). Safranin O staining showed comparable matrix levels between wild type and PEDF-deficient animals in the vehicle control groups, suggesting that the loss of PEDF did not affect the formation of articular cartilage. In particular, cartilage matrix was reduced in MIA-injected wild type knees, but was better preserved in the PEDF-deficient knee (Figure 3.1.6b). When the percent loss of Safranin O staining within the articular cartilage was quantified for MIA-injected knees, the tibia and femur from PEDF-deficient mice were better protected from matrix loss and resulted in better preserved matrix within the joint (Figure 3.1.6c). Using the

Osteoarthritis Research Society International (OARSI) histological scoring system [94], the data of percent loss of Safranin O staining corresponded to OARSI scores that also reflected less damage with PEDF-deficiency (Figure 3.1.6d).

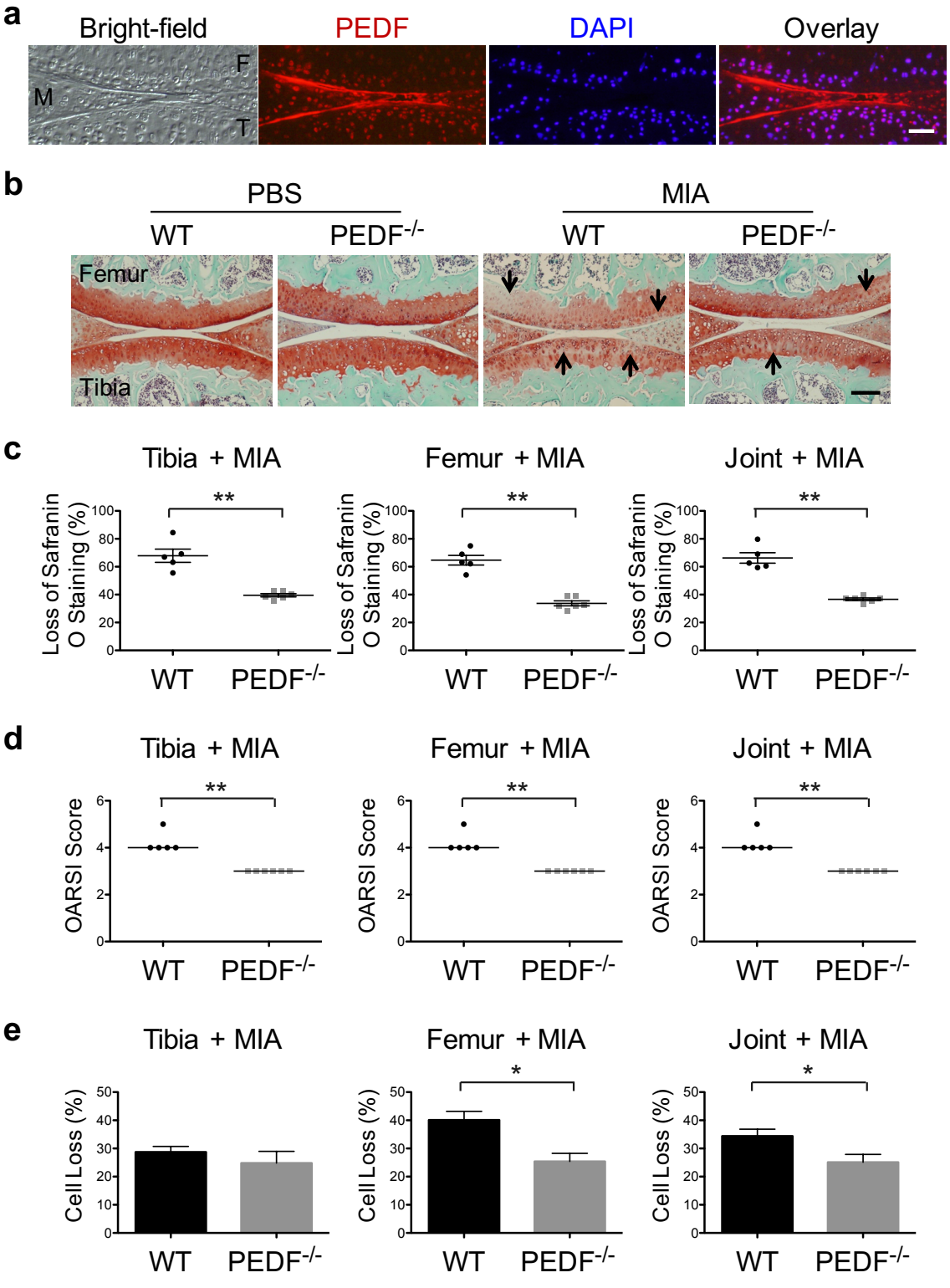

Figure 3.1.6 PEDF-deficiency protects against monosodium iodoacetate (MIA)-induced joint cartilage damage.

(a) PEDF expression was determined via immunofluorescence staining in knee joints from 29 week old wild type animals using a mouse anti-PEDF antibody. Nuclei were counterstained with DAPI. M: meniscus; F: femur; T: tibia. Scale bar = 200μm. (b) MIA or PBS was intraarticularly injected into 29 week old wild type or PEDF-deficient knees, which were harvested after 10 days. Samples were stained with Safranin O and counterstained with Hematoxylin and Fast Green. Arrows indicate areas along the articular surface sustaining a loss of staining. Scale bar = 100μm. (c) The percent area loss of Safranin O staining along the articular surface was calculated for the femur and tibia independently, as well as for the whole joint (femur+tibia). Each point represents the averaged score of an individual animal. Data are plotted as mean ± SEM. (d) OARSI scores were obtained from joint calculations on Safranin O staining. Each point represents an individual animal. The bar represents the median. (e) Quantification of percent cell loss based on DAPI cell counts of the articular surface and empty lacunae. ** $p < 0.01$ (Mann-Whitney test) * $p < 0.05$ (Student's t-test).

We also evaluated the percentage of cell loss based on the previously published analysis method that compared empty lacunae and DAPI staining [88]. While the total cell numbers between wild type and PEDF-deficient knees were not significantly different, cell death was widespread in MIA-treated joints [101-104]. We found a substantial decrease in percent cell loss in PEDF-deficient knees relative to their wild type controls (Figure 3.1.6e). Interestingly, the tibia did not show a significant reduction of cell loss in the PEDF-deficient animal, despite a significant reduction of matrix loss (Figure 3.1.6c). Taken together, these data suggest that PEDF exacerbates cartilage damage in an inflammatory environment and that its presence over time enhances the competence of chondrocytes to respond to inflammatory stimuli.

3.2 Azithromycin and inflammatory joint disease

3.2.1 Azithromycin inhibits cartilage matrix loss *in vivo*

Erythromycin (EM) has previously been shown to exhibit anti-inflammatory activity to slow joint destruction *in vivo* [88]. Because azithromycin (AZM) belongs to the same macrolide class of antibiotics as EM, we hypothesized that it protects against cartilage matrix loss, synovitis and cell loss in an inflammatory joint destruction model *in vivo*. The advantage of azithromycin over erythromycin is the extended half-life of nearly 3 days compared to 3 hours with erythromycin

[77]. To test this hypothesis, we first confirmed that azithromycin can enter the blood stream and penetrate joint tissue. Azithromycin was not found in the serum at either time point from either injection concentration, likely due to the fact that azithromycin is readily taken up by phagocytic cells [78, 79]. While absent from the serum, AZM was found in the knee as early as 1hr post-injection and increased in concentration with increasing dose. Further increases were found at the 6hr time point (Figure 3.2.1). This suggested that azithromycin can penetrate the knee to affect changes within the local joint environment.

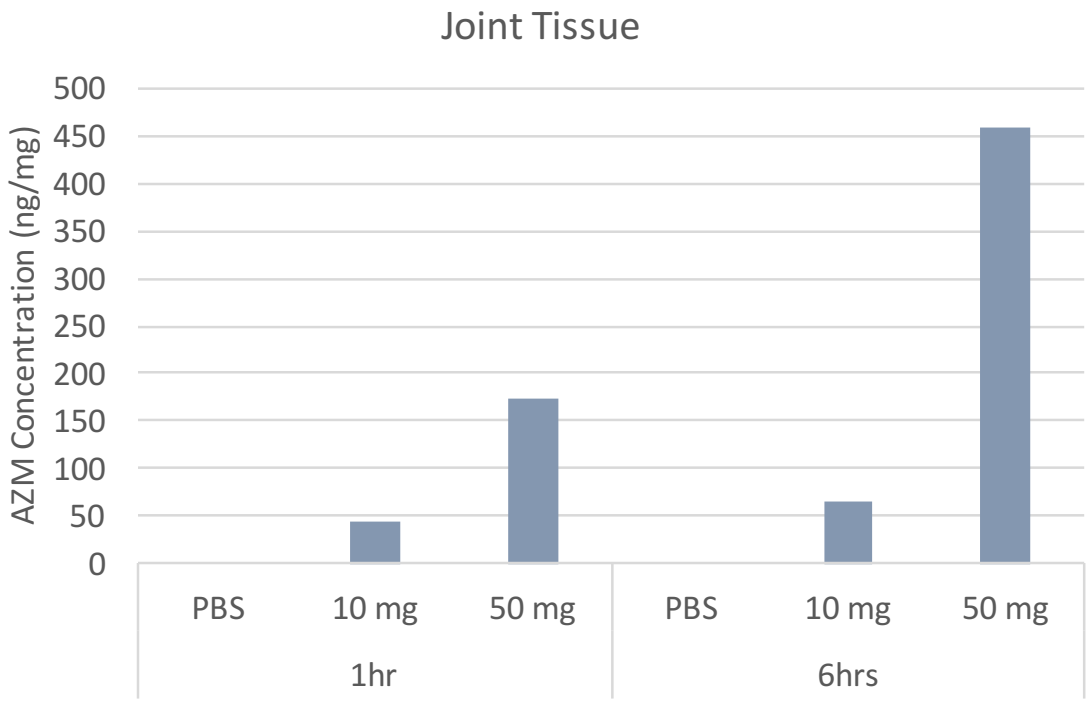

Figure 3.2.1 Azithromycin penetrates joint tissue over time.
C57bl/6 males were given a single subcutaneous injection of azithromycin at either 10 or 50mg/kg or PBS vehicle control. Blood serum and knee joints were isolated 1 and 6hrs post-injection. Azithromycin concentrations were determined by mass spectrometry.

To determine whether azithromycin may exhibit similar anti-inflammatory activity to erythromycin, mice subjected to the monosodium iodoacetate (MIA) inflammatory joint destruction model were treated with daily subcutaneous azithromycin injections. Seven days after MIA injection, knees were harvested for histological analyses. As expected, MIA treatment induced cartilage matrix loss as Safranin O staining along the articular surface was reduced in MIA-injected knees from

mice treated with PBS vehicle control [88]. In animals treated with azithromycin, cartilage matrix was better preserved in the MIA-injected knees (Figure 3.2.2a).

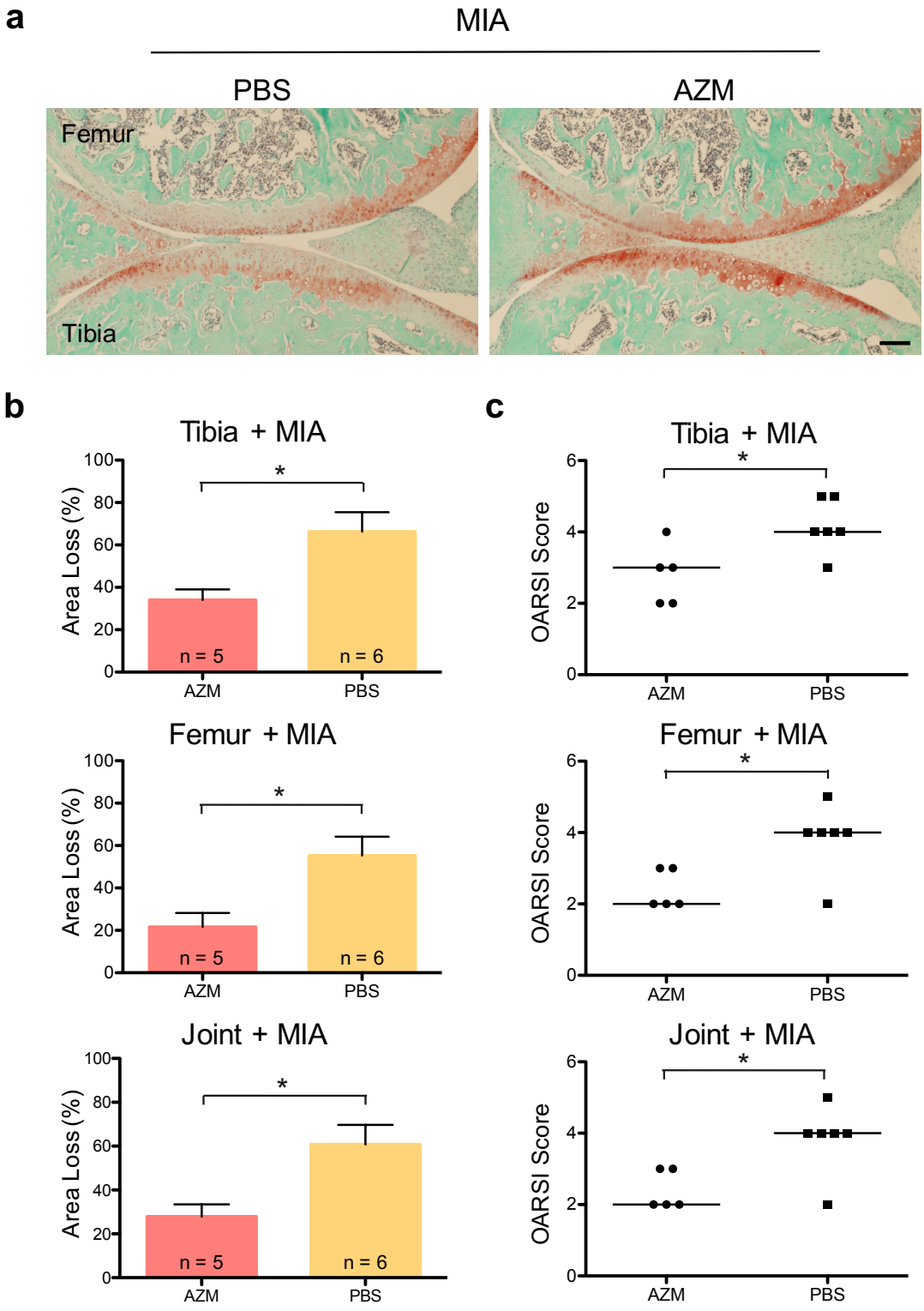

Figure 3.2.2 Azithromycin protects against monosodium iodoacetate (MIA)-induced joint cartilage damage.

(a) MIA was intraarticularly injected into 12 week old C57bl/6 wild type knees and animals received daily subcutaneous injections of azithromycin or vehicle control (PBS). Knees were harvested after 7days and samples were stained with Safranin O and counterstained with Hematoxylin and Fast Green. Scale bar = 50μm. (b) The percent area loss of Safranin O staining along the articular surface was calculated for the femur and tibia independently, as well as for the whole joint (femur+tibia). Data are plotted as mean ± SEM. (c) OARSI scores were obtained from joint calculations on Safranin O staining. Each point represents an individual animal. The bar represents the median. * $p < 0.05$ (Mann-Whitney test).

When the percent area loss of Safranin O staining within the articular cartilage was quantified for the MIA-injected knees, the tibia and femur were better protected from matrix loss and resulted in better preserved matrix within the joint (Figure 3.2.2b). These data corresponded with OARSI scores that also reflected less damage in the azithromycin treated animals (Figure 3.2.2c). These data suggested that azithromycin can not only penetrate knee tissue, but also functionally inhibit the cartilage matrix loss associated with an inflammatory joint destruction model.

Because chondrocyte cell loss is a characteristic feature of arthritic disease, we sought to determine whether cartilage matrix loss was associated with decreased cellularity within the articular surface. Despite preserved cartilage matrix with azithromycin treatment, there were no significant differences between the tibia or the femur cellularity in either the vehicle or azithromycin-treated mice (Figure 3.2.3a-b). Total cell numbers between treatment groups were not significantly different (data not shown).

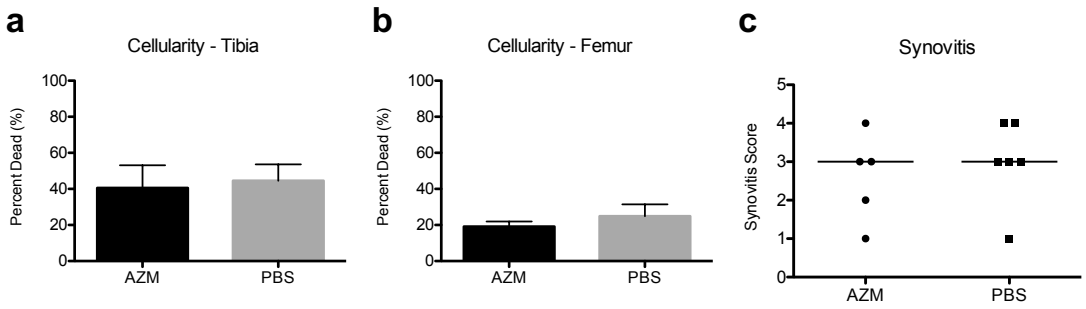

Figure 3.2.3 Azithromycin does not protect against monosodium iodoacetate (MIA)-induced cell loss or synovitis.

(a) Quantification of percent cell loss based on DAPI cell counts of the articular surface and empty lacunae in the tibia of MIA-injected knees from animals treated with either AZM or PBS. (b) Quantification of percent cell loss based on DAPI cell counts of the articular surface and empty lacunae in the femur of MIA-injected knees from animals treated with either AZM or PBS. (c) Synovitis scores determined based on synovium lining and cell density. The bar represents the median.

An additional feature of arthritic disease is synovitis. We used a modified synovitis scoring system, which accounted for cell lining thickness as well as cell density within the synovium [95], as inflammatory infiltrate was not readily seen at this time point. Using the modified system, untreated mice typically scored around 1-2 at baseline (data not shown). In the treated mice, while scores were typically higher, we did not see a significant difference between azithromycin and vehicle treated groups (Figure 3.2.3c).

While azithromycin protected animals from cartilage matrix loss in the inflammatory MIA animal model, it did not affect cellularity or synovitis. This suggested that seven days following MIA injection may not appropriately capture changes in cellularity or synovitis. In fact, significant differences between erythromycin and vehicle control treatment groups in both cellularity and synovitis were previously observed after 10 days of MIA injection [88].

3.2.2 Azithromycin inhibits IL-1β-mediated catabolic gene expression in chondrocytes

To begin addressing the mechanism underlying the protective effects of azithromycin, we sought to model its effects *in vitro* using a chondrocyte cell culture system. RT-PCR analysis on articular cartilage isolated from MIA-injected joints previously showed increased levels of pro-inflammatory cytokine gene expression, such as IL-1β [88]. Because pro-inflammatory cytokines are known to induce catabolic gene expression, we used IL-1β to evaluate the effects of azithromycin on chondrocytes.

We first confirmed that AZM does not induce cell death by measuring its toxicity on primary human articular chondrocytes (NHAC). Cells were plated overnight and treated with increasing doses of AZM the following day for 4 days. Total cell numbers did not significantly differ with increasing AZM concentrations relative to vehicle-treated control cells (Figure 3.2.4a). However, the percentage of dead cells increased significantly relative to the vehicle-treated cells at the 3 and 9μM concentrations (Figure 3.2.4b). Higher azithromycin concentrations of 27 and 81μM would likely be significantly different as well given they exhibit similar percentages of dead cells compared to the 3 and 9μM concentrations; however, the higher variability and relatively low replicate number (n=3) may have influenced whether those higher concentrations were significantly different from the vehicle treated cells. If variability remained the same, increasing replicate number would likely show a difference. Nevertheless, while statistically significant, a seven percentage point increase in cell death relative to vehicle treated cells may not be biologically relevant.

Accordingly, NHAC were pre-treated with increasing concentrations of AZM for 48hrs, followed by challenge with 1ng/mL IL-1β for an additional 48hrs. As expected, IL-1β treatment increased catabolic gene expression. Pre-treatment with AZM inhibited IL-1β-mediated MMP13 and MMP1 induction in a dose-dependent manner (Figure 3.2.4c-d). These data suggest that azithromycin reduces catabolic gene expression induced upon inflammatory challenge.

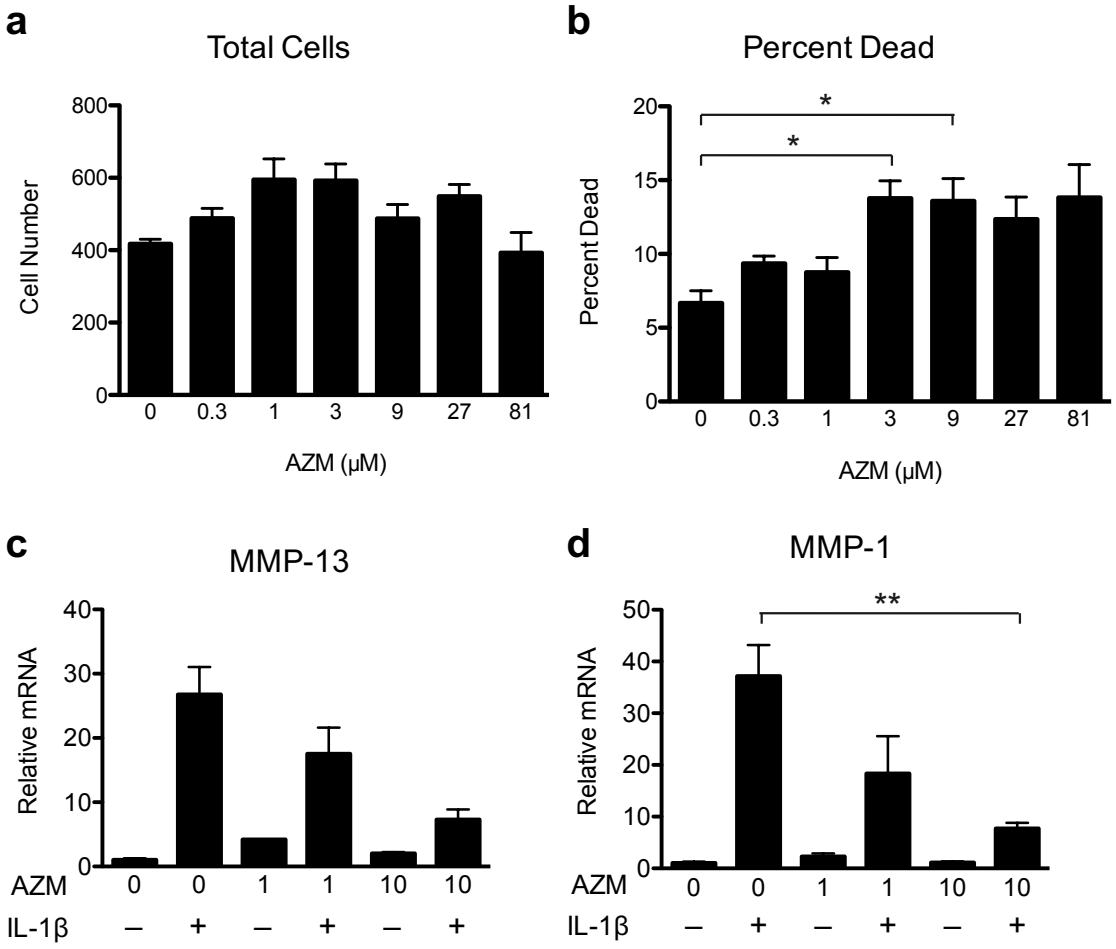

Figure 3.2.4 Azithromycin inhibits IL-1β-mediated catabolic gene expression in normal human articular chondrocytes (NHAC).

(a) Total cell numbers include live and dead cells. (b) Percentage of dead cells were calculated from Ethidium homodimer-1-positive cells relative to total cell number. (c) NHAC were pre-treated with azithromycin for 48hrs followed by inflammatory challenge with 1ng/mL IL-1β for 48hrs. Data are represented as fold change relative to untreated cells in the absence of IL-1β within each gene. Gene expression was normalized to TATA-binding protein mRNA expression levels. Data are plotted as mean ± SEM. Relative MMP-13 gene expression. (d) Relative MMP-1 gene expression. * $p < 0.05$ (Kruskal-Wallis test, Dunn's post-hoc test) ** $p < 0.01$ (Student's t-test)

3.2.3 Anti-inflammatory activity of azithromycin is not mediated by the ghrelin receptor

Because erythromycin has previously been found to function through the ghrelin receptor (unpublished data), we sought to test whether azithromycin may also function through the same

receptor. Growth hormone secretagogue receptor (GHSR) or ghrelin receptor is a G protein-coupled receptor that binds ghrelin to regulate energy homeostasis and body weight. Ghrelin binding to its receptor has been shown to enhance binding to the serum response element (SRE) [105]. Erythromycin was found to bind to the ghrelin receptor and activate downstream signaling through serum response element binding (unpublished data).

To evaluate whether the ghrelin receptor mediates azithromycin activity, immature murine articular chondrocytes (iMAC) from GHSR knockout or wild type littermate mice were pre-treated with azithromycin then challenged with IL-1β. Preliminary studies found 0.1ng/mL IL-1β induced catabolic gene expression (MMP-13) as well as reduced anabolic gene expression (Col-II) (Figure 3.2.5a). Total cell numbers and percentage of dead cells were not significantly different from vehicle control in either wild type or GHSR knockout iMAC, suggesting that azithromycin treatment is not toxic (Figure 3.2.5b-c).

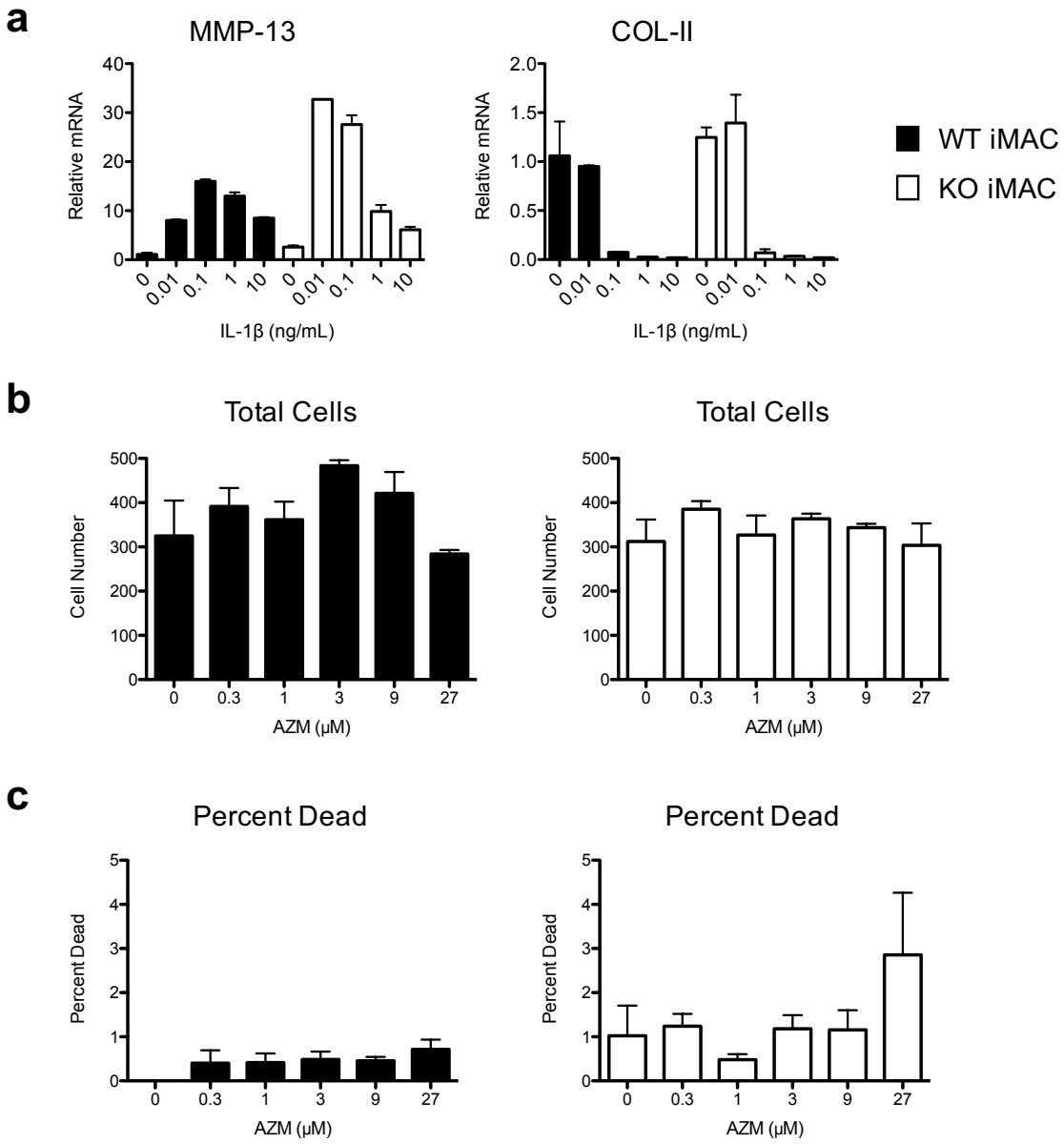

Figure 3.2.5 Preliminary studies establish baseline parameters for immature murine articular chondrocyte (iMAC) culture.

(a) iMAC from wild type or GHSR knockout mice were treated with IL-1β for 48hrs and catabolic and anabolic gene expression was assessed. (b) Total cell numbers include live and dead cells. (c) Percentage of dead cells were calculated from Ethidium homodimer-1-positive cells relative to total cell number.

In the absence of IL-1β, AZM alone did not dramatically increase catabolic gene expression (MMP-13, MMP-3, IL-6). As expected, catabolic gene expression was induced in the presence of IL-1β (Figure 3.2.6a-c). Pre-treatment with AZM attenuated IL-1β-mediated catabolic gene expression in wild type iMAC as similarly observed in NHAC (Figure 3.2.4). These effects were

not abolished in chondrocytes lacking the ghrelin receptor (Figure 3.2.6a-c), suggesting that the anti-inflammatory activity of azithromycin likely involves a mechanism distinct from that of erythromycin.

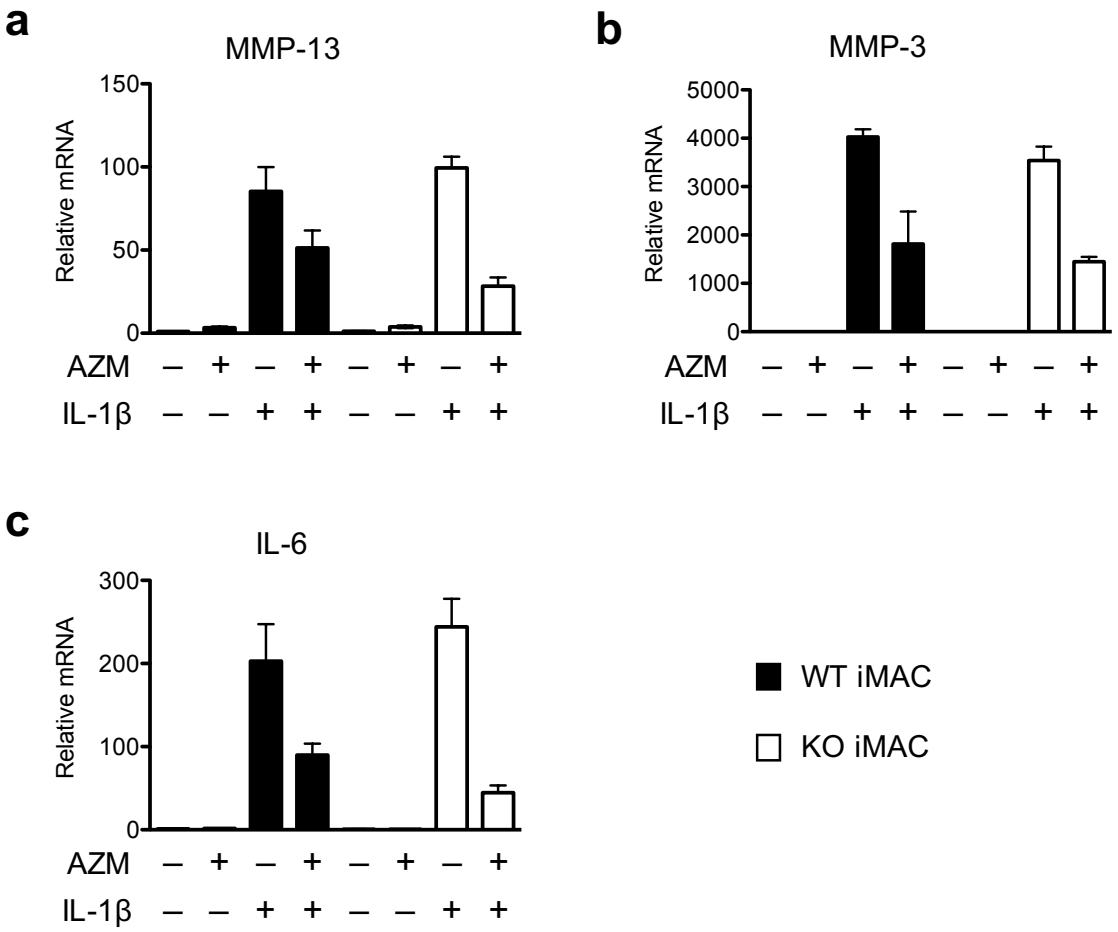

Figure 3.2.6 Anti-inflammatory activity of azithromycin is not mediated by the ghrelin receptor.

Immature murine articular chondrocytes (iMAC) from wild type (WT iMAC) or GHSR knockout (KO iMAC) mice were pre-treated with azithromycin (AZM) for 48hrs followed by challenge with IL-1β for 48hrs. Data are represented as fold change relative to untreated cells in the absence of IL-1β within each gene. Gene expression was normalized to TATA-binding protein mRNA expression levels. Data are plotted as mean ± SEM. (a) Relative MMP-13 gene expression. (b) Relative MMP-3 gene expression. (c) Relative IL-6 gene expression.

3.2.4 Azithromycin does not regulate glucose metabolism in normal human articular chondrocytes challenged with MIA

Because azithromycin inhibited cartilage matrix loss in the inflammatory MIA mouse model and MIA is a specific inhibitor of the glycolytic pathway, we hypothesized that the preserved cartilage matrix resulted from normalized glucose metabolism, as assessed by glucose uptake and glucose consumption We first confirmed that azithromycin did not affect glucose uptake in NHAC (Figure 3.2.7a). We next pre-treated NHAC with AZM for 24hrs, followed by challenge with MIA for 18hrs. MIA inhibited glucose uptake in these 3D cultures; however, AZM was unable to preserve normal glucose uptake in the presence of MIA (Figure 3.2.7b).

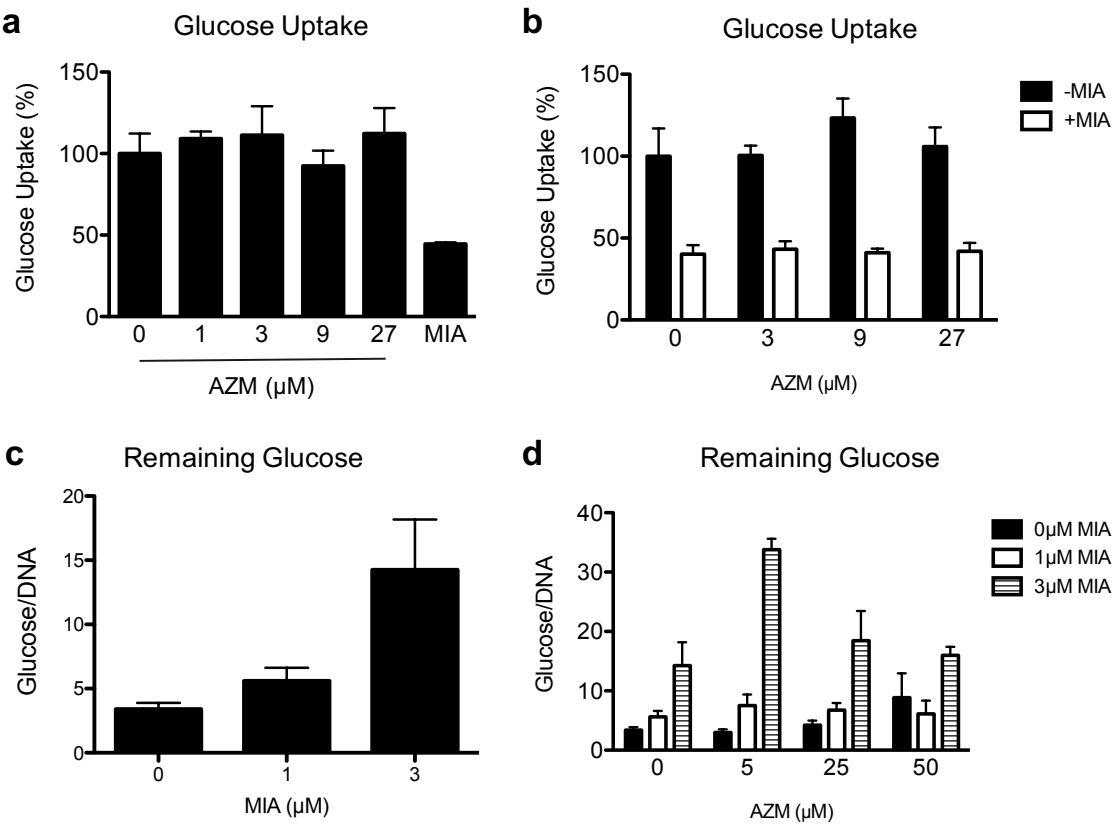

Figure 3.2.7 Azithromycin does not normalize glucose metabolism altered upon MIA treatment.

(a) Normal human articular chondrocytes (NHAC) were treated with increasing concentrations of azithromycin (AZM) and glucose uptake assessed after 24hr incubation. Monosodium iodoacetate (MIA) at 9μM was used as a positive control. (b) NHAC were treated with increasing concentrations of AZM for 24hrs. Glucose uptake was assessed after 18hrs treatment with 9μM MIA. (c) NHAC were treated with MIA for 48hrs and remaining glucose in the culture media was assessed. Glucose concentrations were normalized to end-point DNA content. (d) NHAC were treated with increasing concentrations of AZM for 24hrs, followed by increasing concentrations of MIA for 48hrs. Remaining glucose was assessed to determine glucose consumption.

Because glucose uptake only assesses the internalization of glucose over a short time frame (30 minutes), glucose consumption would offer a better assessment of glucose metabolism over time to determine whether azithromycin may normalize glucose metabolism. To assess glucose consumption, residual glucose in the culture media was assessed after 48hrs treatment with MIA. Remaining glucose values were normalized to end-point DNA content. Higher glucose values are indicative of lower glucose consumption. We first confirmed that MIA reduces glucose consumption in NHAC (Figure 3.2.7c).

We next pre-treated NHAC with AZM for 24hrs, followed by challenge with MIA for 48hrs. In the absence of MIA, glucose consumption appears to decrease with increasing concentrations of AZM; however, this observation is not statistically significant. This slight increase in remaining glucose levels may relate to the elevated toxicity observed with increasing concentrations of AZM (Figure 3.2.4b). In the absence of AZM, MIA dose-dependently reduced glucose consumption in NHAC as previously observed (Figure 3.2.7c). However, none of the AZM concentrations evaluated was able to normalize glucose consumption at any of the MIA concentrations tested (Figure 3.2.7d). In fact, 5μM AZM appears to synergize with 3μM MIA in reducing glucose consumption, which is not observed in other treatment conditions; however, the significance of this finding is unclear. Taken together, these data suggest that the anti-inflammatory activity of azithromycin likely does not involve glucose metabolism normalization. Additional pathways and mechanisms need to be explored to better understand the anti-inflammatory activity of azithromycin in inflammatory joint disease.

4 Discussion and Future Directions

4.1 PEDF under inflammatory conditions

Prior to this work, there were conflicting reports regarding the expression of PEDF in the diseased joint, despite reports of its expression in proliferating and pre-hypertrophic chondrocytes in the growth plate during cartilage development [55]. Our study supports the work of Pfander *et al*, indicating that PEDF is upregulated in articular cartilage under osteoarthritic conditions. Other reports indicate PEDF is also expressed in the bone and promotes osteoblast and osteoclast differentiation; animals with targeted *PEDF* disruption exhibit reduced bone density [66-68, 70]. Its expression in the bone is consistent with that of the osteophyte, the formation of which involves chondrocyte hypertrophy and osteoblast formation [76].

The role of PEDF under inflammatory conditions in cartilage or bone has not been previously explored. Our *in vitro* and *in vivo* studies indicate that PEDF alone does not elicit considerable catabolic activity on cartilage under normal conditions. However, its role is more prominent when chondrocytes are challenged with an inflammatory cytokine, suggesting that PEDF enhances the competence to respond to pro-catabolic factors. This concept of competence in the musculoskeletal system has been observed in normal biology. For example, Parathyroid Hormone-related Protein (PTHrP) can provide competence for a subset of chondrocytes to respond to Indian hedgehog (Ihh) signaling in promoting proliferation [106]. Also, other prochondrogenic signals render chondrocytes competent to activate hypertrophic gene expression in response to Runt-related transcription factor 2 (Runx2) [107]. In the disease state, this concept has been observed in other systems. For instance, glucocorticoids or acute stress sensitize hippocampal microglia to a potentiated pro-inflammatory cytokine response to inflammatory stimuli [108]. Additionally, complement factors induced upon traumatic lung injury have been implicated in priming cells toward enhanced inflammatory responses upon immunologic challenge [109]. However, in the context of arthritis, very little is known about competence toward inflammatory stimuli. We did not observe a difference in IL-1β-induced NF-κB

nuclear localization upon PEDF overexpression; however, PEDF is known to bind extracellular matrix (ECM) components [63-65], which may also mediate cytokine activities. A better understanding of this phenomenon may help to understand the additional compounding factors important in determining the responsiveness or susceptibility of chondrocytes to pro-catabolic factors.

An additional intriguing element is the age-dependent nature of PEDF loss on cartilage integrity under IL-1β treatment. Specifically, PEDF appears to sensitize the cellular response to pro-inflammatory stimuli in aged animals. This is particularly interesting as aging is one of the most prominent risk factors for developing arthritic diseases, but the exact nature of this phenomenon is still not understood. Several reports indicate that age reduces chondrocyte responsiveness to pro-anabolic factors such as insulin-like growth factor 1 (IGF-I) [110-112], and increases susceptibility to osteoarthritis [113], indicating a complicated interplay between aging and inflammation [114]. Consistent with this notion is our observation that cartilage from older wild type bones (29 weeks old) exhibited greater damage compared to younger wild type bones (10 weeks old) upon IL-1β treatment. In particular, PEDF loss prevented this age-related increase in cartilage damage under pro-inflammatory conditions. Thus, it is plausible that PEDF has primed aged chondrocytes to become more responsive to inflammatory stimuli, and suggests that PEDF may lie at the intersection of aging and inflammation to contribute towards joint disease pathogenesis.

The underlying mechanism for our observations is not known. PEDF expression is reduced with age in the skin [115] and retinal pigmented epithelium [116], but elevated in the kidney with age [117]; however, PEDF expression changes in the joint over time is not known. Future studies should determine whether PEDF and PEDF receptor expression changes in the joint with age. Many receptors have been identified for PEDF [93, 118-120], but the particular receptor or set of receptors for PEDF in chondrocytes remains elusive. In particular, it would be interesting to

perform RNA sequencing experiments to identify other players critical in mediating the elevated responsiveness of chondrocytes to catabolic factors. Additionally, evidence in the literature suggests PEDF localizes to the nucleus [121, 122], which we have also seen in our primary human articular chondrocytes. Identifying the particular gene targets, nuclear binding partners or particular receptor(s) involved may begin to reveal the signaling pathways important in eliciting the exacerbated response to inflammatory stimuli and may begin to tease out the mechanisms underlying this observation.

In conclusion, this is the first study to show that PEDF exacerbates cartilage degeneration in an age-dependent manner under an inflammatory setting. This is particularly relevant as age is the greatest risk factor for developing degenerative joint disease; however, we still lack a clear understanding of its role in disease pathogenesis. Our observations suggest that PEDF may prime cells to respond to catabolic factors over time, possibly identifying a molecular link to a prominent risk factor in degenerative joint disease. Our findings identify PEDF as a positive regulator of inflammatory joint disease that possibly links advanced age with increased joint disease prevalence. Further studies could begin to elucidate the mechanism behind one of the most prominent non-modifiable risk factors of joint disease.

4.2 Azithromycin and inflammatory joint disease

Monosodium iodoacetate (MIA) is a known inhibitor of glyceraldehyde-3-phosphate dehydrogenase (GAPDH) [123] and has been shown to induce chondrocyte cell death [101-104]. In fact, we saw significant cell death in primary human articular chondrocytes, demonstrating the high levels of toxicity with MIA treatment (data not shown). Other studies using high concentrations of MIA on primary human osteoblasts nearly completely blocked lactate production after just one hour of treatment [124]. The MIA animal model is thought to induce chondrocyte cell death to disrupt the balance of catabolic and anabolic activities that maintain

cartilage matrix and ultimately leads to joint destruction. It presents with many features characteristic of joint degeneration such as chondrocyte loss, synovial inflammation and bone remodeling [103]. In our animals injected with MIA, we saw a reduction in cartilage matrix. Daily azithromycin (AZM) treatment better preserved the cartilage matrix, which is consistent with erythromycin (EM) treatment. However, azithromycin may be more toxic than EM as lower concentrations of AZM treatment induced higher levels of cell death in NHAC than comparable concentrations with EM (Figure 3.2.4, [88]. Azithromycin even shows a synergistic reduction in glucose consumption with MIA, making it possibly even more toxic to cells at certain concentrations (Figure 3.2.7). Thus, it is not surprising that cellularity did not improve with azithromycin treatment.

As cell survival is unlikely the critical factor involved in cartilage matrix preservation in this model, the early toxic events of MIA treatment may be offset by the anti-inflammatory cytokines produced from remaining surviving cells in response to AZM treatment [125-127]. This could possibly explain the apparently disparate findings of preserved matrix without statistically significant differences observed in cellularity. On the other hand, azithromycin may instead alter cartilage matrix deposition of remaining surviving cells. While we did not see an upregulation of Collagen II or aggrecan gene expression with cells treated with AZM (data not shown), additional studies evaluating matrix deposition would be necessary to evaluate this alternative.

Besides cellularity, resolving synovitis with azithromycin may not be captured by cell lining and density measurements of the synovium. We did not see a difference in the synovitis score between treatment groups, despite previously observed differences on synovitis with EM treatment [88]. It is also unclear when synovitis peaks in this mouse strain. In male Wistar rats, synovitis subsides by day 5 and 7 post-injection [103], whereas NF-κB activity peaks with MIA in Balb/c mice at day 3 post-injection [128]. Additional time points will be necessary to assess for changes in synovitis. It is also possible that the recruitment of cells or the hyperplasia of resident

synoviocytes does not change, but rather the phenotype of the cells that are recruited changes [125-127]. Azithromycin may instead inhibit pro-inflammatory cytokine production and induce anti-inflammatory cytokines, such as IL-10. Cytokine levels should be evaluated with a cytokine array comparing MIA knees of animals treated with AZM or PBS vehicle control [129]. A broader approach using RNA sequencing experiments can help identify other players critical in mediating matrix preservation upon AZM treatment.

Erythromycin has long been known to function as an agonist for the motilin receptor, which is a G protein-coupled receptor involved in gastric migrating myoelectric complexes [130]. Human ghrelin and motilin receptors share 52% overall amino acid identity and 86% in the seven-transmembrane region [130, 131]. However, because the motilin receptor is a pseudogene in murine models [132], ghrelin receptor-mediated activity of erythromycin was confirmed in mouse models lacking ghrelin receptor expression (unpublished data). While EM was shown to function through the ghrelin receptor, azithromycin did not show similar activity despite recent work showing AZM activating the human motilin receptor [133]. This differential activity may result from differential binding of natural peptide ligands and non-peptidyl ligands as was reported for motilin and erythromycin binding to the motilin receptor [132, 134, 135]. Additional studies would need to identify whether azithromycin activity is receptor-mediated or whether other mechanisms of uptake are responsible [132, 136, 137].

Because MIA is a known inhibitor of GAPDH [123], we did see effects of MIA on glucose metabolism in cell cultures. Even at sub-lethal concentrations, glucose consumption was reduced (Figure 3.2.7). However, azithromycin pre-treatment did not normalize glucose consumption despite preserved cartilage matrix with azithromycin treatment *in vivo*. This may highlight the difference between cell culture systems and *in vivo* animal models where cell culture systems simplify complex systems to allow for targeted study. This discrepancy may also reflect the more indirect role of inflammation and cellular recruitment; the direct result of chondrocyte cell death in

response to MIA may lead to indirect consequences of inflammatory cell recruitment. Other signaling pathways may involve anti-inflammatory cytokine production in response to AZM given its extensive literature in other systems [84, 125-127, 138, 139]. For instance, AZM has also been shown to inhibit NF-κB activation following intratracheal LPS challenge [140]. Whether AZM directly induces anti-inflammatory cytokine production in resident joint cells (e.g. chondrocytes, synoviocytes) or whether anti-inflammatory effects are an indirect result of recruited leukocytes are questions that need to be addressed in future studies.

In conclusion, this study builds upon the application of macrolides against the early inflammatory events in joint degeneration. Erythromycin exhibits chondroprotective effects, while azithromycin protects against matrix loss in cartilage in animal models. These findings identify macrolides as a negative regulator of inflammatory joint disease encouraging further development of macrolides as anti-inflammatory therapeutics against inflammatory joint disease progression. In fact, clinical trials with erythromycin in combination with acetaminophen demonstrated functional improvement in osteoarthritis patients [141]. Azithromycin may also join the tetracycline class of antibiotics in exhibiting anti-inflammatory activity [142, 143]. In particular, minocycline appears to be an effective therapy for early rheumatoid arthritis [144] and may suggest other classes of antibiotics offer similar therapeutic potential.

These findings collectively broaden our understanding of both a positive and negative regulator of inflammatory joint disease. With a deeper appreciation of the complexities of disease pathophysiology, we may begin to develop disease modifying therapeutics to combat this expanding unmet clinical need.

5 References

1. Hootman, J.M., et al., *Updated projected prevalence of self-reported doctor-diagnosed arthritis and arthritis-attributable activity limitation among US adults, 2015-2040.* Arthritis Rheumatol, 2016.

2. Yelin, E., et al., *Medical care expenditures and earnings losses among persons with arthritis and other rheumatic conditions in 2003, and comparisons with 1997.* Arthritis Rheum, 2007. **56**(5): p. 1397-407.

3. Centers for Disease, C. and Prevention, *Prevalence of doctor-diagnosed arthritis and arthritis-attributable activity limitation--United States, 2010-2012.* MMWR Morb Mortal Wkly Rep, 2013. **62**(44): p. 869-73.

4. Donahue, K.E., et al., *Systematic review: comparative effectiveness and harms of disease-modifying medications for rheumatoid arthritis.* Ann Intern Med, 2008. **148**(2): p. 124-34.

5. Yu, S.P. and D.J. Hunter, *Emerging drugs for the treatment of knee osteoarthritis.* Expert Opin Emerg Drugs, 2015. **20**(3): p. 361-78.

6. Loeser, R.F., et al., *Osteoarthritis: a disease of the joint as an organ.* Arthritis Rheum, 2012. **64**(6): p. 1697-707.

7. Kiani, C., et al., *Structure and function of aggrecan.* Cell Res, 2002. **12**(1): p. 19-32.

8. Shoulders, M.D. and R.T. Raines, *Collagen structure and stability.* Annu Rev Biochem, 2009. **78**: p. 929-58.

9. Eyre, D., *Collagen of articular cartilage.* Arthritis Res, 2002. **4**(1): p. 30-5.

10. Sophia Fox, A.J., A. Bedi, and S.A. Rodeo, *The basic science of articular cartilage: structure, composition, and function.* Sports Health, 2009. **1**(6): p. 461-8.

11. Hunziker, E.B., T.M. Quinn, and H.J. Hauselmann, *Quantitative structural organization of normal adult human articular cartilage.* Osteoarthritis Cartilage, 2002. **10**(7): p. 564-72.

12. Lin, Z., et al., *The chondrocyte: biology and clinical application.* Tissue Eng, 2006. **12**(7): p. 1971-84.

13. Frank, C.B., *Ligament structure, physiology and function.* J Musculoskelet Neuronal Interact, 2004. **4**(2): p. 199-201.

14. Makris, E.A., P. Hadidi, and K.A. Athanasiou, *The knee meniscus: structure-function, pathophysiology, current repair techniques, and prospects for regeneration.* Biomaterials, 2011. **32**(30): p. 7411-31.

15. Smith, M.D., *The normal synovium.* Open Rheumatol J, 2011. **5**: p. 100-6.

16. Tamer, T.M., *Hyaluronan and synovial joint: function, distribution and healing.* Interdiscip Toxicol, 2013. **6**(3): p. 111-25.

17. Tonge, D.P., M.J. Pearson, and S.W. Jones, *The hallmarks of osteoarthritis and the potential to develop personalised disease-modifying pharmacological therapeutics.* Osteoarthritis Cartilage, 2014. **22**(5): p. 609-21.

18. Sohn, D.H., et al., *Plasma proteins present in osteoarthritic synovial fluid can stimulate cytokine production via Toll-like receptor 4.* Arthritis Res Ther, 2012. **14**(1): p. R7.

19. Bugatti, S., et al., *B cells in rheumatoid arthritis: from pathogenic players to disease biomarkers.* Biomed Res Int, 2014. **2014**: p. 681678.

20. McInnes, I.B. and G. Schett, *The pathogenesis of rheumatoid arthritis.* N Engl J Med, 2011. **365**(23): p. 2205-19.

21. Burmester, G.R., E. Feist, and T. Dorner, *Emerging cell and cytokine targets in rheumatoid arthritis.* Nat Rev Rheumatol, 2014. **10**(2): p. 77-88.

22. Wojdasiewicz, P., L.A. Poniatowski, and D. Szukiewicz, *The role of inflammatory and anti-inflammatory cytokines in the pathogenesis of osteoarthritis.* Mediators Inflamm, 2014. **2014**: p. 561459.

23. Kapoor, M., et al., *Role of proinflammatory cytokines in the pathophysiology of osteoarthritis.* Nat Rev Rheumatol, 2011. **7**(1): p. 33-42.

24. Garlanda, C., C.A. Dinarello, and A. Mantovani, *The interleukin-1 family: back to the future.* Immunity, 2013. **39**(6): p. 1003-18.

25. Dinarello, C.A., A. Simon, and J.W. van der Meer, *Treating inflammation by blocking interleukin-1 in a broad spectrum of diseases.* Nat Rev Drug Discov, 2012. **11**(8): p. 633-52.

26. Furman, B.D., et al., *Targeting pro-inflammatory cytokines following joint injury: acute intra-articular inhibition of interleukin-1 following knee injury prevents post-traumatic arthritis.* Arthritis Res Ther, 2014. **16**(3): p. R134.

27. Joosten, L.A., et al., *IL-1 alpha beta blockade prevents cartilage and bone destruction in murine type II collagen-induced arthritis, whereas TNF-alpha blockade only ameliorates joint inflammation.* J Immunol, 1999. **163**(9): p. 5049-55.

28. Joosten, L.A., et al., *Anticytokine treatment of established type II collagen-induced arthritis in DBA/1 mice. A comparative study using anti-TNF alpha, anti-IL-1 alpha/beta, and IL-1Ra.* Arthritis Rheum, 1996. **39**(5): p. 797-809.

29. Palmer, G., et al., *Mice transgenic for intracellular interleukin-1 receptor antagonist type 1 are protected from collagen-induced arthritis.* Eur J Immunol, 2003. **33**(2): p. 434-40.

30. Fan, Z., et al., *Freshly isolated osteoarthritic chondrocytes are catabolically more active than normal chondrocytes, but less responsive to catabolic stimulation with interleukin-1beta.* Arthritis Rheum, 2005. **52**(1): p. 136-43.

31. Mengshol, J.A., et al., *Interleukin-1 induction of collagenase 3 (matrix metalloproteinase 13) gene expression in chondrocytes requires p38, c-Jun N-terminal kinase, and nuclear factor kappaB: differential regulation of collagenase 1 and collagenase 3.* Arthritis Rheum, 2000. **43**(4): p. 801-11.

32. Reboul, P., et al., *The new collagenase, collagenase-3, is expressed and synthesized by human chondrocytes but not by synoviocytes. A role in osteoarthritis.* J Clin Invest, 1996. **97**(9): p. 2011-9.

33. Tetlow, L.C., D.J. Adlam, and D.E. Woolley, *Matrix metalloproteinase and proinflammatory cytokine production by chondrocytes of human osteoarthritic cartilage: associations with degenerative changes.* Arthritis Rheum, 2001. **44**(3): p. 585-94.

34. Little, C.B., et al., *Matrix metalloproteinase 13-deficient mice are resistant to osteoarthritic cartilage erosion but not chondrocyte hypertrophy or osteophyte development.* Arthritis Rheum, 2009. **60**(12): p. 3723-33.

35. de Lange-Brokaar, B.J., et al., *Synovial inflammation, immune cells and their cytokines in osteoarthritis: a review.* Osteoarthritis Cartilage, 2012. **20**(12): p. 1484-99.

36. Chevalier, X., et al., *Intraarticular injection of anakinra in osteoarthritis of the knee: a multicenter, randomized, double-blind, placebo-controlled study.* Arthritis Rheum, 2009. **61**(3): p. 344-52.

37. Cohen, S.B., et al., *A randomized, double-blind study of AMG 108 (a fully human monoclonal antibody to IL-1R1) in patients with osteoarthritis of the knee.* Arthritis Res Ther, 2011. **13**(4): p. R125.

38. Bresnihan, B., et al., *Treatment of rheumatoid arthritis with recombinant human interleukin-1 receptor antagonist.* Arthritis Rheum, 1998. **41**(12): p. 2196-204.

39. Matsuno, H., et al., *The role of TNF-alpha in the pathogenesis of inflammation and joint destruction in rheumatoid arthritis (RA): a study using a human RA/SCID mouse chimera.* Rheumatology (Oxford), 2002. **41**(3): p. 329-37.

40. Bradley, J.R., *TNF-mediated inflammatory disease.* J Pathol, 2008. **214**(2): p. 149-60.

41. Sedger, L.M. and M.F. McDermott, *TNF and TNF-receptors: From mediators of cell death and inflammation to therapeutic giants - past, present and future.* Cytokine Growth Factor Rev, 2014. **25**(4): p. 453-72.

42. Moelants, E.A., et al., *Regulation of TNF-alpha with a focus on rheumatoid arthritis.* Immunol Cell Biol, 2013. **91**(6): p. 393-401.

43. Lubberts, E., et al., *Adenoviral vector-mediated overexpression of IL-4 in the knee joint of mice with collagen-induced arthritis prevents cartilage destruction.* J Immunol, 1999. **163**(8): p. 4546-56.

44. van Lent, P.L., et al., *Local overexpression of adeno-viral IL-4 protects cartilage from metallo proteinase-induced destruction during immune complex-mediated arthritis by preventing activation of pro-MMPs.* Osteoarthritis Cartilage, 2002. **10**(3): p. 234-43.

45. van Meegeren, M.E., et al., *IL-4 alone and in combination with IL-10 protects against blood-induced cartilage damage.* Osteoarthritis Cartilage, 2012. **20**(7): p. 764-72.

46. Yeh, L.A., et al., *Interleukin-4, an inhibitor of cartilage breakdown in bovine articular cartilage explants.* J Rheumatol, 1995. **22**(9): p. 1740-6.

47. Cush, J.J., et al., *Elevated interleukin-10 levels in patients with rheumatoid arthritis.* Arthritis Rheum, 1995. **38**(1): p. 96-104.

48. Greenhill, C.J., et al., *Interleukin-10 regulates the inflammasome-driven augmentation of inflammatory arthritis and joint destruction.* Arthritis Res Ther, 2014. **16**(4): p. 419.

49. Iannone, F., et al., *Interleukin-10 and interleukin-10 receptor in human osteoarthritic and healthy chondrocytes.* Clin Exp Rheumatol, 2001. **19**(2): p. 139-45.

50. Finnegan, A., et al., *Collagen-induced arthritis is exacerbated in IL-10-deficient mice.* Arthritis Res Ther, 2003. **5**(1): p. R18-24.

51. Walmsley, M., et al., *Interleukin-10 inhibition of the progression of established collagen-induced arthritis.* Arthritis Rheum, 1996. **39**(3): p. 495-503.

52. Tombran-Tink, J., G.G. Chader, and L.V. Johnson, *PEDF: a pigment epithelium-derived factor with potent neuronal differentiative activity.* Exp Eye Res, 1991. **53**(3): p. 411-4.

53. Steele, F.R., et al., *Pigment epithelium-derived factor: neurotrophic activity and identification as a member of the serine protease inhibitor gene family.* Proc Natl Acad Sci U S A, 1993. **90**(4): p. 1526-30.

54. He, X., et al., *PEDF and its roles in physiological and pathological conditions: implication in diabetic and hypoxia-induced angiogenic diseases.* Clin Sci (Lond), 2015. **128**(11): p. 805-23.

55. Quan, G.M., et al., *Localization of pigment epithelium-derived factor in growing mouse bone.* Calcif Tissue Int, 2005. **76**(2): p. 146-53.

56. Chetty, A., et al., *Pigment epithelium-derived factor mediates impaired lung vascular development in neonatal hyperoxia.* Am J Respir Cell Mol Biol, 2015. **52**(3): p. 295-303.

57. Hoshina, D., et al., *The role of PEDF in tumor growth and metastasis.* Curr Mol Med, 2010. **10**(3): p. 292-5.

58. Manalo, K.B., et al., *Pigment epithelium-derived factor as an anticancer drug and new treatment methods following the discovery of its receptors: a patent perspective.* Expert Opin Ther Pat, 2011. **21**(2): p. 121-30.

59. Becerra, S.P. and V. Notario, *The effects of PEDF on cancer biology: mechanisms of action and therapeutic potential.* Nat Rev Cancer, 2013. **13**(4): p. 258-71.

60. Rychli, K., K. Huber, and J. Wojta, *Pigment epithelium-derived factor (PEDF) as a therapeutic target in cardiovascular disease.* Expert Opin Ther Targets, 2009. **13**(11): p. 1295-302.

61. Liu, J.T., et al., *Role of pigment epithelium-derived factor in stem/progenitor cell-associated neovascularization.* J Biomed Biotechnol, 2012. **2012**: p. 871272.

62. Yabe, T., T. Sanagi, and H. Yamada, *The neuroprotective role of PEDF: implication for the therapy of neurological disorders.* Curr Mol Med, 2010. **10**(3): p. 259-66.

63. Alberdi, E., C.C. Hyde, and S.P. Becerra, *Pigment epithelium-derived factor (PEDF) binds to glycosaminoglycans: analysis of the binding site.* Biochemistry, 1998. **37**(30): p. 10643-52.

64. Meyer, C., L. Notari, and S.P. Becerra, *Mapping the type I collagen-binding site on pigment epithelium-derived factor. Implications for its antiangiogenic activity.* J Biol Chem, 2002. **277**(47): p. 45400-7.

65. Becerra, S.P., et al., *Pigment epithelium-derived factor binds to hyaluronan. Mapping of a hyaluronan binding site.* J Biol Chem, 2008. **283**(48): p. 33310-20.

66. Gattu, A.K., et al., *Determination of mesenchymal stem cell fate by pigment epithelium-derived factor (PEDF) results in increased adiposity and reduced bone mineral content.* FASEB J, 2013. **27**(11): p. 4384-94.

67. Li, F., et al., *Pigment epithelium-derived factor enhances differentiation and mineral deposition of human mesenchymal stem cells.* Stem Cells, 2013. **31**(12): p. 2714-23.

68. Bogan, R., et al., *A mouse model for human osteogenesis imperfecta type VI.* J Bone Miner Res, 2013. **28**(7): p. 1531-6.

69. Li, F., et al., *Pigment epithelium derived factor suppresses expression of Sost/Sclerostin by osteocytes: implication for its role in bone matrix mineralization.* J Cell Physiol, 2015. **230**(6): p. 1243-9.

70. Akiyama, T., et al., *PEDF regulates osteoclasts via osteoprotegerin and RANKL.* Biochem Biophys Res Commun, 2010. **391**(1): p. 789-94.

71. Zhang, S.X., et al., *Pigment epithelium-derived factor (PEDF) is an endogenous antiinflammatory factor.* FASEB J, 2006. **20**(2): p. 323-5.

72. Wang, J.J., et al., *Anti-inflammatory effects of pigment epithelium-derived factor in diabetic nephropathy.* Am J Physiol Renal Physiol, 2008. **294**(5): p. F1166-73.

73. Famulla, S., et al., *Pigment epithelium-derived factor (PEDF) is one of the most abundant proteins secreted by human adipocytes and induces insulin resistance and inflammatory signaling in muscle and fat cells.* Int J Obes (Lond), 2011. **35**(6): p. 762-72.

74. Yabe, T., et al., *Pigment epithelium-derived factor induces pro-inflammatory genes in neonatal astrocytes through activation of NF-kappa B and CREB.* Glia, 2005. **50**(3): p. 223-34.

75. Pfander, D., et al., *Pigment epithelium derived factor--the product of the EPC-1 gene--is expressed by articular chondrocytes and up regulated in osteoarthritis.* Ann Rheum Dis, 2006. **65**(7): p. 965-7.

76. Klinger, P., et al., *The Transient Chondrocyte Phenotype in Human Osteophytic Cartilage: A Role of Pigment Epithelium-Derived Factor?* Cartilage, 2013. **4**(3): p. 249-55.

77. Whitman, M.S. and A.R. Tunkel, *Azithromycin and clarithromycin: overview and comparison with erythromycin.* Infect Control Hosp Epidemiol, 1992. **13**(6): p. 357-68.

78. McDonald, P.J. and H. Pruul, *Phagocyte uptake and transport of azithromycin.* Eur J Clin Microbiol Infect Dis, 1991. **10**(10): p. 828-33.

79. Bosnar, M., et al., *Cellular uptake and efflux of azithromycin, erythromycin, clarithromycin, telithromycin, and cethromycin.* Antimicrob Agents Chemother, 2005. **49**(6): p. 2372-7.

80. Vallee, E., et al., *Activity and local delivery of azithromycin in a mouse model of Haemophilus influenzae lung infection.* Antimicrob Agents Chemother, 1992. **36**(7): p. 1412-7.

81. Gladue, R.P., et al., *In vitro and in vivo uptake of azithromycin (CP-62,993) by phagocytic cells: possible mechanism of delivery and release at sites of infection.* Antimicrob Agents Chemother, 1989. **33**(3): p. 277-82.

82. Girard, A.E., C.R. Cimochowski, and J.A. Faiella, *Correlation of increased azithromycin concentrations with phagocyte infiltration into sites of localized infection.* J Antimicrob Chemother, 1996. **37 Suppl C**: p. 9-19.

83. Schultz, M.J., *Macrolide activities beyond their antimicrobial effects: macrolides in diffuse panbronchiolitis and cystic fibrosis.* J Antimicrob Chemother, 2004. **54**(1): p. 21-8.

84. Ratzinger, F., et al., *Azithromycin suppresses CD4(+) T-cell activation by direct modulation of mTOR activity.* Sci Rep, 2014. **4**: p. 7438.

85. Sugiyama, K., et al., *Differing effects of clarithromycin and azithromycin on cytokine production by murine dendritic cells.* Clin Exp Immunol, 2007. **147**(3): p. 540-6.

86. Meyer, M., et al., *Azithromycin reduces exaggerated cytokine production by M1 alveolar macrophages in cystic fibrosis.* Am J Respir Cell Mol Biol, 2009. **41**(5): p. 590-602.

87. Alzolibani, A.A. and K. Zedan, *Macrolides in chronic inflammatory skin disorders.* Mediators Inflamm, 2012. **2012**: p. 159354.

88. Uchimura, T., et al., *The Chondroprotective Role of Erythromycin in a Murine Joint Destruction Model.* Cartilage, 2016.

89. van der Sluijs, J.A., et al., *The reliability of the Mankin score for osteoarthritis.* J Orthop Res, 1992. **10**(1): p. 58-61.

90. Livak, K.J. and T.D. Schmittgen, *Analysis of relative gene expression data using real-time quantitative PCR and the 2(-Delta Delta C(T)) Method.* Methods, 2001. **25**(4): p. 402-8.

91. Chen, Y., et al., *Validation of a PicoGreen-based DNA quantification integrated in an RNA extraction method for two-dimensional and three-dimensional cell cultures.* Tissue Eng Part C Methods, 2012. **18**(6): p. 444-52.

92. Huang, Q., et al., *PEDF-deficient mice exhibit an enhanced rate of retinal vascular expansion and are more sensitive to hyperoxia-mediated vessel obliteration.* Exp Eye Res, 2008. **87**(3): p. 226-41.

93. Park, K., et al., *Identification of a novel inhibitor of the canonical Wnt pathway.* Mol Cell Biol, 2011. **31**(14): p. 3038-51.

94. Glasson, S.S., et al., *The OARSI histopathology initiative - recommendations for histological assessments of osteoarthritis in the mouse.* Osteoarthritis Cartilage, 2010. **18 Suppl 3**: p. S17-23.

95. Krenn, V., et al., *Synovitis score: discrimination between chronic low-grade and high-grade synovitis.* Histopathology, 2006. **49**(4): p. 358-64.

96. Gosset, M., et al., *Primary culture and phenotyping of murine chondrocytes.* Nat Protoc, 2008. **3**(8): p. 1253-60.

97. van der Sluijs, J.A., C.W. Thesingh, and J.P. Scherft, *Skin inhibits cartilage proliferation and calcification. Tissue culture of fetal mice bones.* Acta Orthop Scand, 1986. **57**(6): p. 518-22.

98. Klement, B.J. and B.S. Spooner, *Embryonic mouse pre-metatarsal development in organ culture.* J Exp Zool, 1993. **265**(3): p. 285-94.

99. Song, W., et al., *The fetal mouse metatarsal bone explant as a model of angiogenesis.* Nat Protoc, 2015. **10**(10): p. 1459-73.

100. Landman, E.B., et al., *Small molecule inhibitors of WNT/beta-catenin signaling block IL-1beta- and TNFalpha-induced cartilage degradation.* Arthritis Res Ther, 2013. **15**(4): p. R93.

101. Grossin, L., et al., *Induction of heat shock protein 70 (Hsp70) by proteasome inhibitor MG 132 protects articular chondrocytes from cellular death in vitro and in vivo.* Biorheology, 2004. **41**(3-4): p. 521-34.

102. Barve, R.A., et al., *Transcriptional profiling and pathway analysis of monosodium iodoacetate-induced experimental osteoarthritis in rats: relevance to human disease.* Osteoarthritis Cartilage, 2007. **15**(10): p. 1190-8.

103. Guzman, R.E., et al., *Mono-iodoacetate-induced histologic changes in subchondral bone and articular cartilage of rat femorotibial joints: an animal model of osteoarthritis.* Toxicol Pathol, 2003. **31**(6): p. 619-24.

104. Guingamp, C., et al., *Mono-iodoacetate-induced experimental osteoarthritis: a dose-response study of loss of mobility, morphology, and biochemistry.* Arthritis Rheum, 1997. **40**(9): p. 1670-9.

105. Liu, G., et al., *Four missense mutations in the ghrelin receptor result in distinct pharmacological abnormalities.* J Pharmacol Exp Ther, 2007. **322**(3): p. 1036-43.

106. Karp, S.J., et al., *Indian hedgehog coordinates endochondral bone growth and morphogenesis via parathyroid hormone related-protein-dependent and -independent pathways.* Development, 2000. **127**(3): p. 543-8.

107. Kempf, H., et al., *Prochondrogenic signals induce a competence for Runx2 to activate hypertrophic chondrocyte gene expression.* Dev Dyn, 2007. **236**(7): p. 1954-62.

108. Frank, M.G., et al., *Glucocorticoids mediate stress-induced priming of microglial pro-inflammatory responses.* Brain Behav Immun, 2012. **26**(2): p. 337-45.

109. Hoth, J.J., et al., *Complement mediates a primed inflammatory response after traumatic lung injury.* J Trauma Acute Care Surg, 2014. **76**(3): p. 601-8; discussion 608-9.

110. Loeser, R.F., et al., *Reduction in the chondrocyte response to insulin-like growth factor 1 in aging and osteoarthritis: studies in a non-human primate model of naturally occurring disease.* Arthritis Rheum, 2000. **43**(9): p. 2110-20.

111. Loeser, R.F., et al., *Aging and oxidative stress reduce the response of human articular chondrocytes to insulin-like growth factor 1 and osteogenic protein 1.* Arthritis Rheumatol, 2014. **66**(8): p. 2201-9.

112. Martin, J.A., S.M. Ellerbroek, and J.A. Buckwalter, *Age-related decline in chondrocyte response to insulin-like growth factor-I: the role of growth factor binding proteins.* J Orthop Res, 1997. **15**(4): p. 491-8.

113. Loeser, R.F., et al., *Microarray analysis reveals age-related differences in gene expression during the development of osteoarthritis in mice.* Arthritis Rheum, 2012. **64**(3): p. 705-17.

114. Greene, M.A. and R.F. Loeser, *Aging-related inflammation in osteoarthritis.* Osteoarthritis Cartilage, 2015. **23**(11): p. 1966-71.

115. Francis, M.K., et al., *Loss of EPC-1/PEDF expression during skin aging in vivo.* J Invest Dermatol, 2004. **122**(5): p. 1096-105.

116. Steinle, J.J., S. Sharma, and V.C. Chin, *Normal aging involves altered expression of growth factors in the rat choroid.* J Gerontol A Biol Sci Med Sci, 2008. **63**(2): p. 135-40.

117. Pina, A.L., et al., *Expression of pigment-epithelium-derived factor during kidney development and aging.* Cell Tissue Res, 2007. **329**(2): p. 329-38.

118. Notari, L., et al., *Identification of a lipase-linked cell membrane receptor for pigment epithelium-derived factor.* J Biol Chem, 2006. **281**(49): p. 38022-37.

119. Bernard, A., et al., *Laminin receptor involvement in the anti-angiogenic activity of pigment epithelium-derived factor.* J Biol Chem, 2009. **284**(16): p. 10480-90.

120. Notari, L., et al., *Pigment epithelium-derived factor binds to cell-surface F(1)-ATP synthase.* FEBS J, 2010. **277**(9): p. 2192-205.

121. Tombran-Tink, J., et al., *Expression, secretion, and age-related downregulation of pigment epithelium-derived factor, a serpin with neurotrophic activity.* J Neurosci, 1995. **15**(7 Pt 1): p. 4992-5003.

122. Anguissola, S., et al., *Pigment epithelium-derived factor (PEDF) interacts with transportin SR2, and active nuclear import is facilitated by a novel nuclear localization motif.* PLoS One, 2011. **6**(10): p. e26234.

123. Schmidt, M.M. and R. Dringen, *Differential effects of iodoacetamide and iodoacetate on glycolysis and glutathione metabolism of cultured astrocytes.* Front Neuroenergetics, 2009. **1**: p. 1.

124. Duewelhenke, N., O. Krut, and P. Eysel, *Influence on mitochondria and cytotoxicity of different antibiotics administered in high concentrations on primary human osteoblasts and cell lines.* Antimicrob Agents Chemother, 2007. **51**(1): p. 54-63.

125. Munic, V., et al., *Intensity of macrolide anti-inflammatory activity in J774A.1 cells positively correlates with cellular accumulation and phospholipidosis.* Pharmacol Res, 2011. **64**(3): p. 298-307.

126. Vrancic, M., et al., *Azithromycin distinctively modulates classical activation of human monocytes in vitro.* Br J Pharmacol, 2012. **165**(5): p. 1348-60.

127. Murphy, B.S., et al., *Azithromycin alters macrophage phenotype.* J Antimicrob Chemother, 2008. **61**(3): p. 554-60.

128. Bowles, R.D., et al., *In vivo luminescence imaging of NF-kappaB activity and serum cytokine levels predict pain sensitivities in a rodent model of osteoarthritis.* Arthritis Rheumatol, 2014. **66**(3): p. 637-46.

129. Shen, P.C., et al., *T helper cells promote disease progression of osteoarthritis by inducing macrophage inflammatory protein-1gamma.* Osteoarthritis Cartilage, 2011. **19**(6): p. 728-36.

130. Sanger, G.J. and J.B. Furness, *Ghrelin and motilin receptors as drug targets for gastrointestinal disorders.* Nat Rev Gastroenterol Hepatol, 2016. **13**(1): p. 38-48.

131. Peeters, T., et al., *Erythromycin is a motilin receptor agonist.* Am J Physiol, 1989. **257**(3 Pt 1): p. G470-4.

132. De Smet, B., A. Mitselos, and I. Depoortere, *Motilin and ghrelin as prokinetic drug targets.* Pharmacol Ther, 2009. **123**(2): p. 207-23.

133. Broad, J. and G.J. Sanger, *The antibiotic azithromycin is a motilin receptor agonist in human stomach: comparison with erythromycin.* Br J Pharmacol, 2013. **168**(8): p. 1859-67.

134. Matsuura, B., M. Dong, and L.J. Miller, *Differential determinants for peptide and non-peptidyl ligand binding to the motilin receptor. Critical role of second extracellular loop for peptide binding and action.* J Biol Chem, 2002. **277**(12): p. 9834-9.

135. Matsuura, B., et al., *Differential contributions of motilin receptor extracellular domains for peptide and non-peptidyl agonist binding and activity.* J Biol Chem, 2006. **281**(18): p. 12390-6.

136. Montenez, J.P., et al., *Interaction of the macrolide azithromycin with phospholipids. II. Biophysical and computer-aided conformational studies.* Eur J Pharmacol, 1996. **314**(1-2): p. 215-27.

137. Montenez, J.P., et al., *Interactions of macrolide antibiotics (Erythromycin A, roxithromycin, erythromycylamine [Dirithromycin], and azithromycin) with phospholipids: computer-aided conformational analysis and studies on acellular and cell culture models.* Toxicol Appl Pharmacol, 1999. **156**(2): p. 129-40.

138. Ivetic Tkalcevic, V., et al., *Anti-inflammatory activity of azithromycin attenuates the effects of lipopolysaccharide administration in mice.* Eur J Pharmacol, 2006. **539**(1-2): p. 131-8.

139. Parnham, M.J., et al., *Azithromycin: mechanisms of action and their relevance for clinical applications.* Pharmacol Ther, 2014. **143**(2): p. 225-45.

140. Stellari, F.F., et al., *Azithromycin inhibits nuclear factor-kappaB activation during lung inflammation: an in vivo imaging study.* Pharmacol Res Perspect, 2014. **2**(5): p. e00058.

141. Sadreddini, S., et al., *A double blind, randomized, placebo controlled study to evaluate the efficacy of erythromycin in patients with knee effusion due to osteoarthritis.* Int J Rheum Dis, 2009. **12**(1): p. 44-51.

142. Di Caprio, R., et al., *Anti-inflammatory properties of low and high doxycycline doses: an in vitro study.* Mediators Inflamm, 2015. **2015**: p. 329418.

143. Bernardino, A.L., D. Kaushal, and M.T. Philipp, *The antibiotics doxycycline and minocycline inhibit the inflammatory responses to the Lyme disease spirochete Borrelia burgdorferi.* J Infect Dis, 2009. **199**(9): p. 1379-88.

144. O'Dell, J.R., et al., *Treatment of early seropositive rheumatoid arthritis with minocycline: four-year followup of a double-blind, placebo-controlled trial.* Arthritis Rheum, 1999. **42**(8): p. 1691-5.